

Doctoral Dissertation

**The Reconfigurable Maze System for Studying the Neural
Underpinning of Spatial Cognition and Navigation**

Satoshi Hoshino

Graduate School of Brain Science, Doshisha University

A thesis submitted for the degree of

Doctor of Philosophy in Science

Mar. 2022

Abstract

All animals, including humans, have the ability to recognize space and navigate to a destination. To clarify the mechanisms of navigation behavior, animal behavioral experiments often use mazes of various shapes, including the T-maze, cross-maze, figure-8 maze, and radial arm maze. However, conventional maze experiments are conducted in different laboratories, which could cause alterations in the activities of neurons, including place cells in the hippocampus, resulting in difficulties to compare existing maze experiments. Therefore, in this study, we developed a reconfigurable maze system consisting of rearrangeable runways and an array of accompanying parts to achieve multiple maze shapes in a single laboratory. By arranging the parts along the grid pattern, the desired maze shape can be reproduced by any researcher. While achieving a high degree of freedom in the maze shape, there is a spatial gap between any pair of parts to prevent physical interference between them. When we examined the effect of this gap on navigation behavior, we found no difference in animal behavior with or without the gap. Similarly, for the activity of place cells in the hippocampus, we found no effect of the gap on the number and length of spatial receptive fields, the average firing frequency of multiunit activity, or the accuracy of location estimation by place cell activity. To demonstrate the effectiveness of the reconfigurable maze system, we constructed two mazes, one square and one cross-shaped, in a single environment, and trained rats to run clockwise through each maze. Although the total distance of the runway of the maze did not change during its deformation, the location of the spatial receptive field was remapped, suggesting that the maze shape influences spatial cognition and navigation. Thus, the reconfigurable maze enables comparative studies by reproduce

multiple shape maze in a single environment, and provides a consistent experimental setup for elucidating spatial cognition and navigational abilities.

Acknowledgments

I would like to express my deepest gratitude to my mentor, Dr. Susumu Takahashi, for his continuous guidance, scientific advice, and encouragement over the past five years. I am grateful to Dr. Kaoru Ide, Dr. Hirotsugu Azechi, Mr. Riku Takahashi, Ms. Kana Mieino, Mr. Yuta Tamatsu, and all the other members of my laboratory for their encouragement and insightful comments regarding this research. Without them, this research would not have been possible. I would like to give special thanks to my thesis committee members, Dr. Yoshio Sakurai, Dr. Nobuyuki Nukina, and Dr. Jun Motoyama, for their cooperation and efforts during my examination. Finally, I would like to express my sincere gratitude to my family for their understanding, support, and encouragement. Without their dedication, I would not have been able to undertake and complete this study.

Table of Contents

1. Introduction.....	- 9 -
1.1. Animal behavioral experiments using mazes.....	- 9 -
1.2. Conventional maze experiments are poorly comparable	- 13 -
1.3. Maze experiments and place cells.....	- 15 -
1.4. Remapping of the place fields.....	- 17 -
1.5. Disadvantages of animal behavioral experiments using virtual reality (VR)	- 18 -
1.6. Purpose	- 20 -
2. Materials and Methods.....	- 22 -
2.1. Maze system implementation.....	- 22 -
2.2. Animals	- 23 -
2.3. Surgery, electrode preparation, and recording.....	- 24 -
2.4. Behavioral training	- 25 -
2.5. Morphing experiment	- 26 -
2.6. Spatial alternation task	- 27 -
2.7. Animal trajectory and head direction	- 27 -
2.8. Behavioral and neural analyses.....	- 27 -
2.9. Statistical analyses.....	- 30 -
2.10. Histology	- 31 -
3. Results	- 32 -
3.1. Implementation of the reconfigurable maze.....	- 32 -

3.2. Interlocking gaps do not alter navigational behavior	- 35 -
3.3. Interlocking gaps do not alter hippocampal place coding	- 42 -
3.4. Rats can learn spatial alternation tasks in the reconfigured maze	- 45 -
3.5. Place field remapping during the maze morphing experiment.....	- 47 -
4. Discussion.....	- 52 -
4.1. Neural recording from freely moving rats	- 52 -
4.2. Limitations of reproducible maze shapes	- 53 -
4.3. Morphing runways causes remapping of the place fields	- 54 -
4.4. Standardization of maze experiments	- 54 -
4.5. Future Studies	- 55 -
5. References	- 57 -

List of figures and tables

Figures

Figure 1-1 Hampton Court Maze

Figure 1-2 Schematic diagram of the two radial arm maze experiments

Figure 1-3 Schematic diagram of the maze experiment in the laboratory

Figure 1-4 Examples of place cells in a corridor maze

Figure 1-5 Vector-based navigation and deep learning models

Figure 1-6 Remapping of the receptive field

Figure 1-7 Navigational experiment using virtual reality

Figure 3-1 Maze reproduced by the reconfigurable maze

Figure 3-2 Interlocking mechanisms and accompanying parts

Figure 3-3 Assembly time of the reconfigurable maze for morphing the shape from square to cruciform

Figure 3-4 A short gap between runways is a prerequisite margin for the interlocking parts.

Figure 3-5 Schematics of the square-shaped maze test

Figure 3-6 Running speed and head direction on the runway with or without gaps

Figure 3-7 Square-shaped maze test with long runways

Figure 3-8 Occupancy time over the maze

Figure 3-9 Place cells and lengths of the receptive fields

Figure 3-10 Number of place fields and firing rate of multiunit activity

Figure 3-11 Estimation of the rats' position

Figure 3-12 Learning of the spatial alternation tasks

Figure 3-13 Maze morphing experiment

Figure 3-14 Place cells in the morphing experiment

Figure 3-15 Spatial similarity and rate similarity

Figure 3-16 More examples of place cells

Tables

Table 1-1 Maze shapes and research objectives

Table 2-1 Dimensions of the runway of the reconfigurable maze

Table 2-2 Variability between rats: electrophysiological measurements

1. Introduction

Various animal species, including humans, have the ability to navigate to a destination by locating themselves and responding to changes in their environment. To illustrate this ability, Tolman proposed the cognitive map hypothesis, in which the mind contains a map of the immediate environment (Tolman, 1948). Currently, the cognitive map is thought to be composed of spatial cognitive cells in the brain, such as place cells, which represent one's location (O'Keefe and Dostrovsky, 1971), and grid cells, which represent the distance to a specific direction (Fyhn *et al.*, 2004).

Various behavioral experiments have been devised to test a subject's navigational ability. To make animals perform the desired navigation behaviors, mazes with specialized shapes have been developed and used.

1.1. Animal behavioral experiments using mazes

Animal experiments using mazes have a long history, dating back to the beginning of the last century. The early maze was modeled after the Hampton Court maze in England to study the navigation behavior of animals in a complex maze (Vincent, 1915; Figure 1-1). Since then, the T-maze (Tolman and Gleitman, 1949), radial arm maze (Olton and Samuelson, 1976), W-maze (Frank, Brown and Wilson, 2000), and multiple T-maze (Lohninger, Strasser and Bubna-Littitz, 2001) have been devised, and animal behavioral experiments have been conducted. Although maze experiments began from the study of spatial navigation, they were also used to investigate neurophysiological mechanisms other than spatial cognition (Table 1-1).

The experimental effectiveness of a given maze shape depends on the experimental variables that can be manipulated and the neurophysiological mechanisms that can be examined. For example, the radial arm maze is traditionally used to test the mechanisms of spatial learning and memory. Olton and Samuelson developed an early version of this maze in which food was placed at each end of eight radially arranged runways (Figure 1-2, left). The animals were placed in the center of the maze and were free to explore until all pellets were collected. The optimal strategy in this maze is to visit each passage once, and the number of re-entries to the same passage is used to quantify the degree of spatial working memory. In the radial arm maze, a simple variant experiment was conducted. In this experiment, pellets were placed in only four predetermined arms out of eight arms. In addition to the spatial working memory of which arm pellets have already been retrieved, the animal must retain the spatial reference memory of which arms receive pellets (Figure 1-2, right). Thus, an advantage of the corridor maze is that various experiments can be performed by manipulating some of the variables.

An obvious advantage of animal experiments that utilize mazes is their ability to limit the movement of animals to a specific path. In animal experiments, simple trials are often repeated to obtain a quantitative picture of the changes in animal behavior caused by experimental variables. By using a corridor-type maze, we can maintain the speed, direction, and distance of an animal's motion within a certain range. In addition, we can control the sensory inputs, such as visual and tactile sensations that the animals experience, to ensure that these do not vary from trial to trial. The corridor-type is useful for verifying how specific experimental manipulations affect animal behavior. Therefore, it is expected that more animal behavior experiments using

various mazes will be conducted in the future (Igata, Sasaki and Ikegaya, 2016).

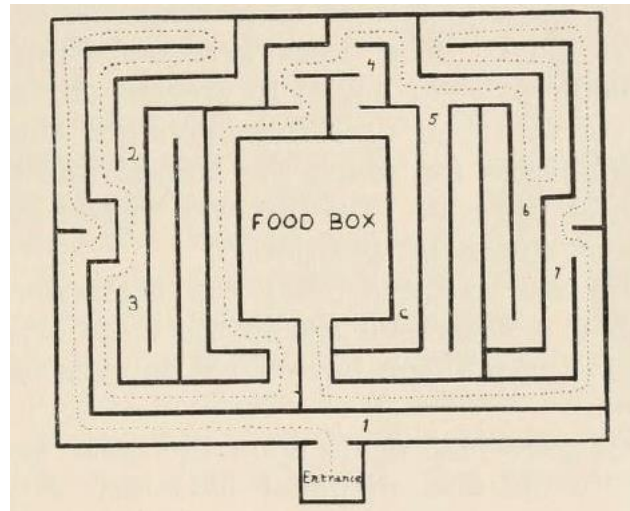
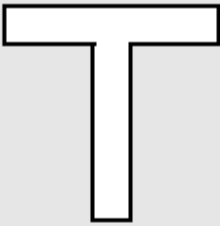
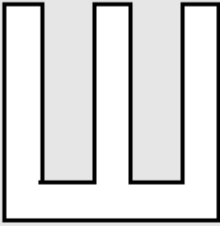
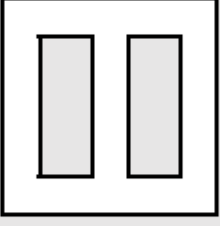
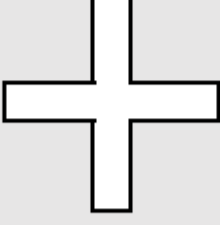



Figure 1-1 Hampton Court Maze

Dotted lines indicate the shortest path. Numbers indicate dead-end aisles. Adapted from Vincent 1915.

Table 1-1 Maze shapes and research objectives

Maze	Schematic	Objective
T-maze		Place coding Decision making Motivation
W-maze		Place coding
Figure-8 maze		Place coding Time coding Episodic memory
Plus maze		Place coding Anxiety
Radial arm maze		Place coding Learning and memory

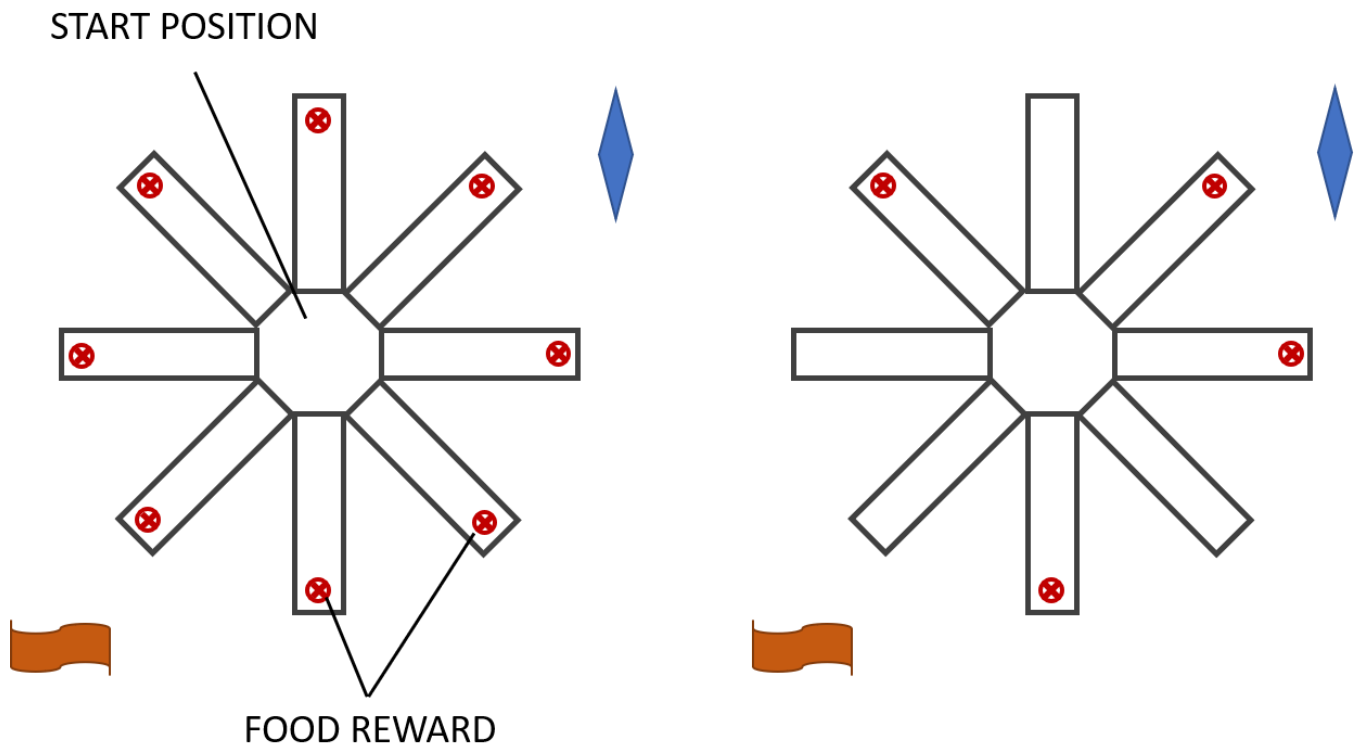


Figure 1-2 Schematic diagram of the two radial arm maze experiments

Blue diamond and orange flags are distal visual cues. The left panel demonstrates a spatial memory experiment. Rats are initially placed in the central octagonal stage, and they explore the maze until they obtain the rewards from all eight arms. The right panel demonstrates a separation experiment of spatial short-term memory and spatial working memory. Rewards are placed only in some predetermined passages among the eight passages. Rats need to retain both spatial short-term memory of which passages contain rewards and the spatial working memory regarding the passages from they have already retrieved treats.

1.2. Conventional maze experiments are poorly comparable

A wide variety of maze experiments have been conducted, and neurophysiological data on spatial cognition and navigation are being accumulated. However, even a maze of the same shape may yield different experimental results when the experimental setup is different. For example, it has been reported that neural representations of animal locations are modified by maze scale, maze proximal cues (e.g., color and material of the maze), and maze distal cues (e.g., size, walls, and lighting of the laboratory), respectively. Therefore, the results of these experiments depend on the maze setup and may not be reproducible (Figures 1-3, A-D; detailed in subsection 1.4.).

Moreover, interpreting neural mechanisms using only one experimental system may lead to misinterpretations (Sharma, Rakoczy and Brown-Borg, 2010), and it is necessary to comprehensively analyze the results of multiple shapes of maze. However, as mentioned earlier, the experimental results in the maze depend on scale, proximal cues, and distal cues, respectively, so ideally, these experiments should be performed in a single experimental setup (Figure 1-3, E).

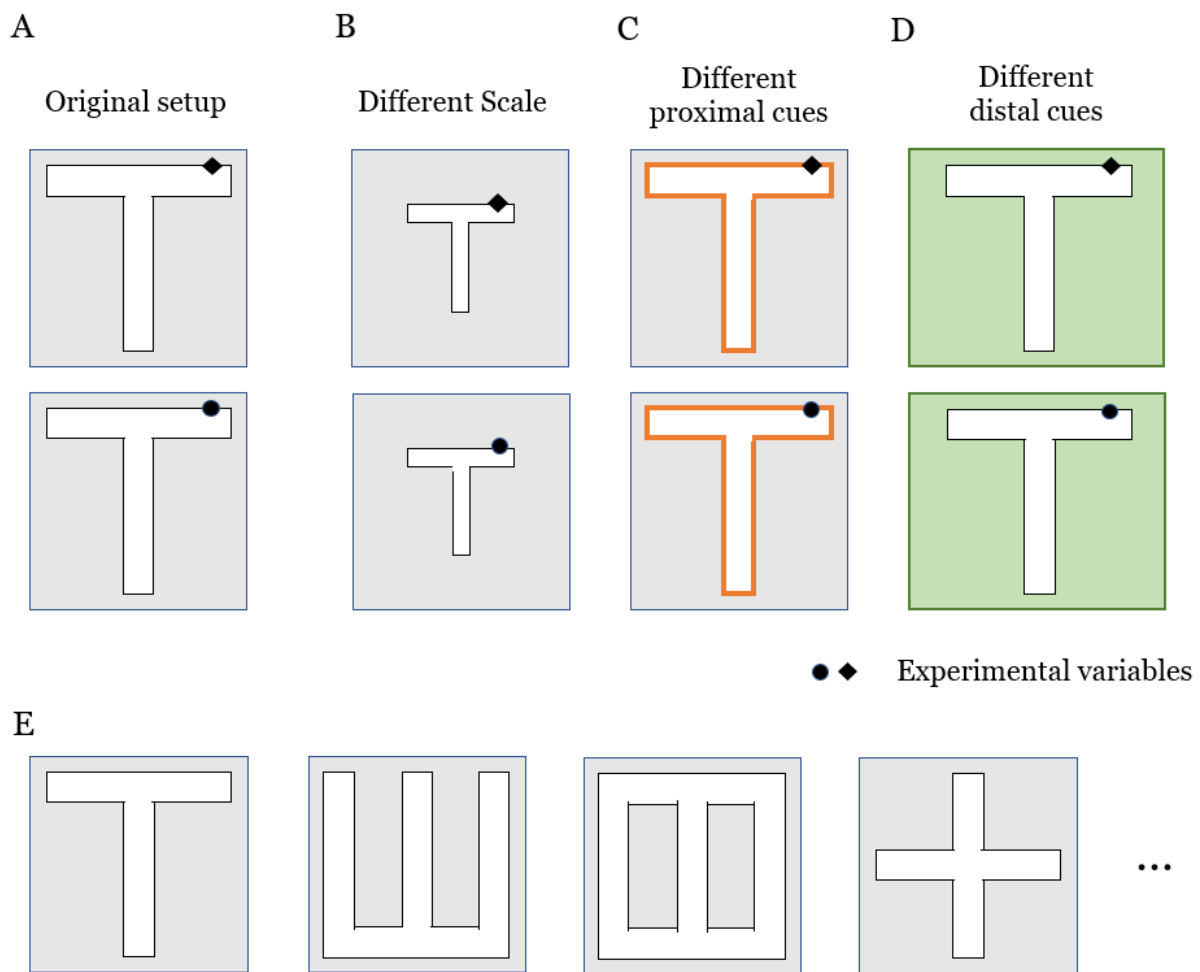


Figure 1-3 Schematic diagram of the maze experiment in the laboratory

(A-D) The same type of experiment is performed in different setups. Even a simple T-maze experiment may yield different results if the scale of the maze (B), proximal cues (C, e.g., color and material of the maze), and distal cues (D, e.g., size, walls, and lighting of the laboratory) are different.

(E) Ideally, all maze experiments should be conducted with the same scale, proximal cues, and distal cues.

1.3. Maze experiments and place cells

Behavioral experiments using mazes involve the movement of animals. This means that the maze test always includes the process of spatial cognition in experimental animals. The study of spatial cognition in animals is an essential component of maze experiments.

O'Keefe and Dostrovsky recorded neuronal activity in the hippocampus of rats running free in an open field and reported cells that fire when the animal passed a specific location (O'Keefe and Dostrovsky, 1971). Because the firing position of a cell depends on the position of the animal, regardless of the speed and orientation of the animal, cells with such properties are called place cells. The animal location for which the action potential is generated is different for each cell, and the location where each cell fires is called the place receptive field of the place cell. In the hippocampal CA1 region, 30% to 50% of pyramidal cells are place cells (Muller, Kubie and Ranck, 1987), and they cover the entire environment, which may support Tolman's cognitive map hypothesis. The activity of place cells in the corridor maze has also been investigated, and it has been found that cells with place receptive fields are present throughout the experimental apparatus as in the open field (Figure 1-4).

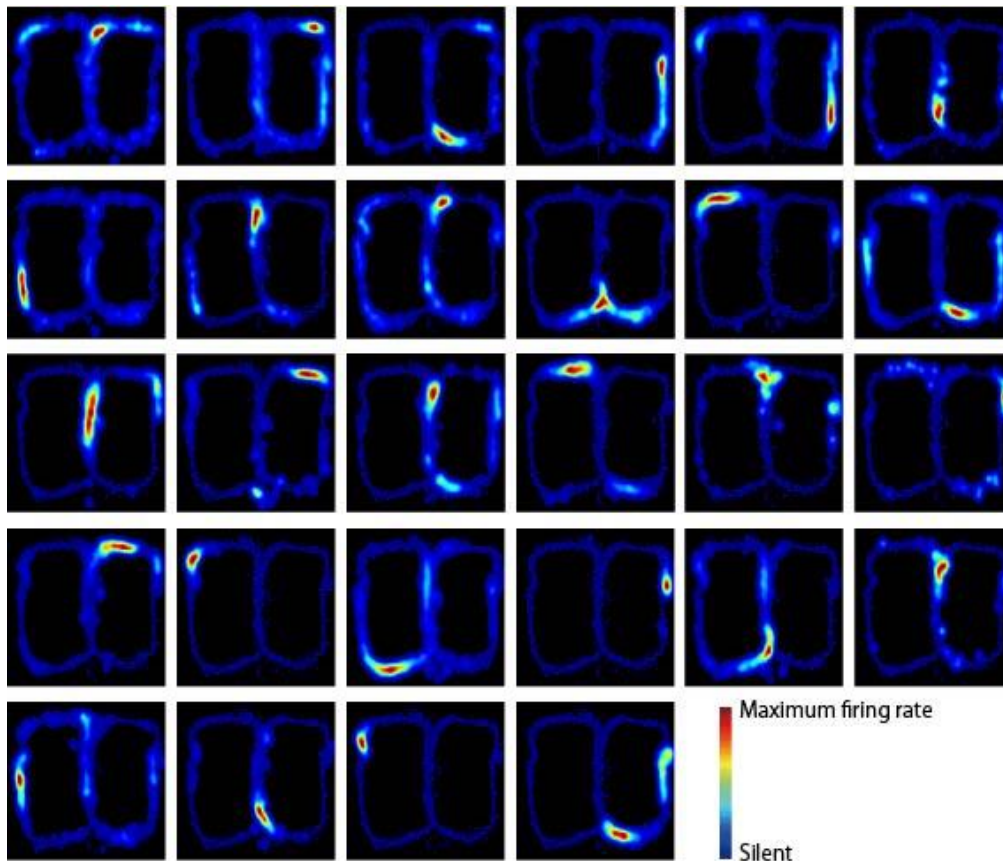


Figure 1-4 Examples of place cells in a corridor maze

In each figure, the color represents the average firing rate of the hippocampal pyramidal cells in each location. The deeper the red color, the higher the firing frequency. In this example, the animal is performing a task in which it moves from the bottom to the top of the central passage and then selects the left or right direction. Adapted from the Dictionary of Neuroscience.

(<https://bsd.neuroinf.jp/wiki/%E5%A0%B4%E6%89%80%E7%B4%B0%E8%83%9E>)

The hippocampus is also closely related to the navigation behavior in animals. In humans, this was suggested by a report of a unique volume increase in the hippocampus of London cab drivers (Maguire *et al.*, 2000). In hippocampal disruption experiments in rats, it has been reported that navigation behavior is impaired when the maze environment is changed (Winocur *et al.*, 2010). Furthermore, a recent modeling study using deep learning have successfully allowed agents to navigate complex environments (Banino *et al.*, 2018). It is believed that grid cell activity is

necessary to plan actions by calculating vectors between the current location and the destination (vector-based navigation), and the authors report the generation of grid cell-like activity in the middle layer using the firing of place and head direction cells as training data (Figure 1-5).

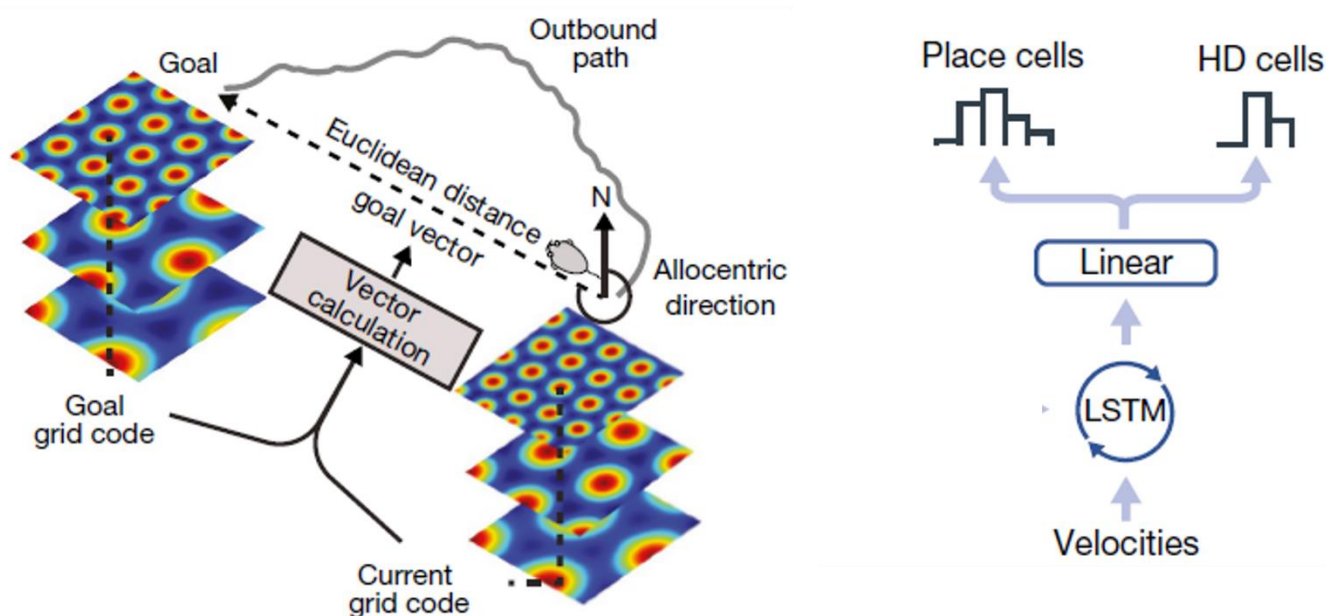


Figure 1-5 Vector-based navigation and deep learning models

Left, vector-based navigation. A vector from the current location to the destination is calculated using the activities of grid cells of different scales. Right, deep learning model. LSTM indicates recurrent network with a long short-term memory. The network uses velocity data to compute the firing of place cells and head direction cells (HD cells). After learning was complete, some of linear layer units showed a firing pattern like grid cells. Modified from Banino *et al.*, 2018.

1.4. Remapping of the place fields

The neural representation of space in the hippocampus has been found to change partially or completely in response to proximal or distal cues (these are collectively called the external cues).

This phenomenon is called remapping of the place fields. Hippocampal place cells often undergo large changes in the firing patterns in response to small changes in the experimental environment (Figure 1-6). For example, changes in external factors, such as the shape and size of the experimental container (Muller and Kubie, 1987), brightness and darkness of the room

(Quirk, Muller and Kubie, 1990), and color of the container (Bostock, Muller and Kubie, 1991) are known to cause remapping. Even if the external stimuli are the same, internal changes such as motivation (Kennedy and Shapiro, 2009), past experience or future destinations (Wood *et al.*, 2000), and the content of the current task (Takahashi, 2013) can cause remapping of the place field.

Remapping is thought to serve the function of pattern separation, in which similar but not identical experiences show different neural representations (Colgin, Moser and Moser, 2008). It has been suggested that remapping is extremely sensitive to changes in the environment and produces different cognitive maps in different rooms, even when the same maze shape is reproduced in different rooms (Leutgeb *et al.*, 2005). Therefore, it is necessary to transform the maze in the same room and in the same place when comparing neural activities in multiple maze experiments.

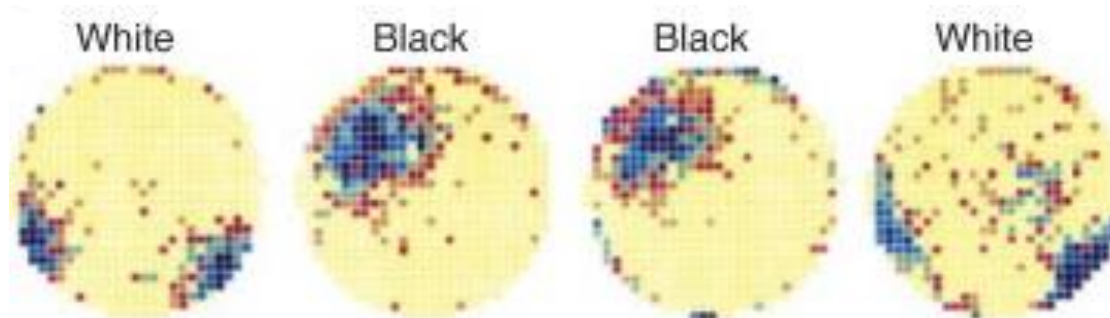


Figure 1-6 Remapping of the receptive field

Rats search for food in a circular arena. The average firing rate of the pyramidal cells is shown in color. Yellow indicates no firing, and the average firing rate increases as the color changes from red to blue. In this example, the location of the receptive field changes in response to changes in the color of the arena. Adapted from Bostock, Muller and Kubie, 1991.

1.5. Disadvantages of animal behavioral experiments using virtual reality (VR)

Behavioral experiments using virtual reality (VR) can be considered to simulate a maze consisting of arbitrary shapes in a single environment. Behavioral experiments using VR technology were first conducted in humans and then applied to animal experiments. One of the earliest applications in rodents was the study of spatial navigation using visual VR. This was a behavioral experiment in which rodents acquired food by reaching the source of a cylindrical visual cue in a virtual open field space (Hölscher *et al.*, 2005; Figure 1-7, left). There have also been many VR experiments using corridor mazes. One example is an experiment in which rats had to perform a visual discrimination task in a virtual T-maze (Harvey, Coen and Tank, 2012).

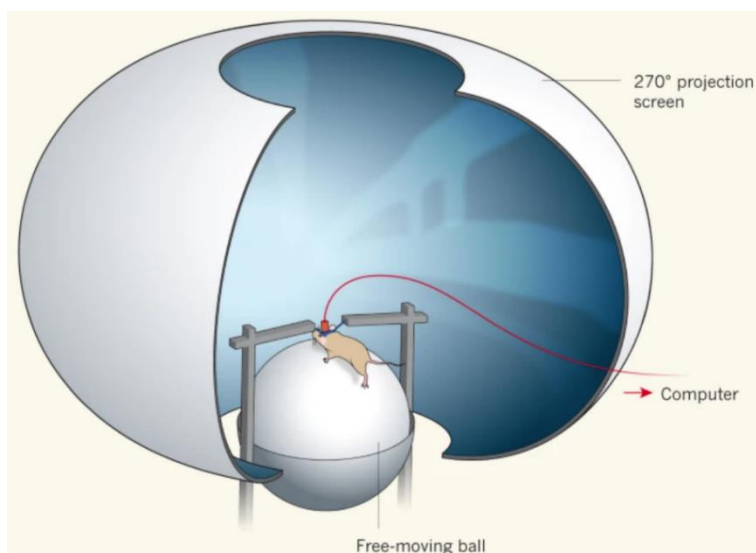
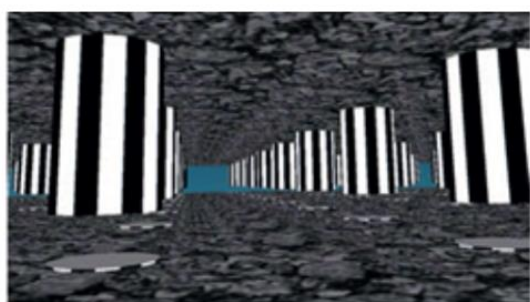


Figure 1-7 Navigational experiment using virtual reality

Left, virtual space explored by a rat. Moving to the bottom of the striped cylinder earns a reward (Thurley and Ayaz, 2017). Right, a typical VR implementation. The rat is fixed on a Styrofoam sphere whose resistance is reduced by air. The animal's movements are detected using a computer mouse, which is used to update the image of the virtual space. A virtual image is projected onto a circular screen using mirror reflection (Minderer *et al.*, 2016).

The motivation for applying VR to animal experiments is to use it in conjunction with recent technologies for recording neuronal activity. In a typical implementation of VR, the animal's head was fixed against the experimental setup to keep the animal's position constant (Figure 1-7, right). This setup is advantageous when utilizing recording techniques that require the

animal's head position to be fixed. For example, recording of intramembrane potentials using patch clamping (Harvey *et al.*, 2009) and optical detection of neuronal activity using two-photon calcium imaging (Dombeck *et al.*, 2010) have been used in conjunction with VR behavioral experiments.

However, in VR experiments with fixed vestibular sensory stimulation, it has been reported that the percentage of hippocampal pyramidal cells that fire in the environment is reduced (Ravassard *et al.*, 2013). Similarly, visual VR of a single modality lacks tactile and other sensory stimuli and may have an unknown effect on the neuronal activity associated with spatial cognition, including hippocampal place cells. Behavioral experiments with auditory VR (Cushman *et al.*, 2013) and tactile VR (Sofroniew *et al.*, 2014) have already been conducted, but true VR, which presents all sensory inputs simultaneously, is yet to be developed. Therefore, in behavioral experiments using VR, alteration in neuronal activity cannot be excluded.

1.6. Purpose

As we have seen, the maze experiment is a complex experiment that involves neural processes of spatial cognition. Since the experimental results depend on the scale of the maze, proximal cues, and distal cues respectively, experiments using the same shape of the maze may give different results. For the same reason, a simple comparison and discussion of previous studies of multiple mazes may lead to misinterpretation. Therefore, a maze system that realizes multiple maze shapes while keeping scale, proximal cues, and distal cues all similar is required.

In this study, we developed a reconfigurable maze, which is a maze system that can provide

various existing maze by combining simple parts. In the following sections, animal behaviors and hippocampal neuronal activities were verified to demonstrate that the reconfigurable maze actually reproduces existing maze shapes and can be used for animal behavioral experiments.

2. Materials and Methods

2.1. Maze system implementation

The reconfigurable maze consists of interlocking runways (49 cm × 10 cm, see Table 2-1) and an array of accompanying parts including feeders, movable walls, shut-off sensors, and treadmills. Each runway was placed atop a tower mounted on a breadboard with a grid of holes (hole-to-hole spacing: 25 mm), which enabled each section to be mounted independent of other runway sections. Each runway made of 5 mm thick black polyvinyl chloride (PVC) (matte finish) was positioned 55 cm above the breadboard (Table 2-1). The tower and its baseplate were made of aluminum. The baseplate has four protrusions that can be inserted into the holes of the breadboard in order to attach it. Sidewalls (45 mm height) around the top of the runway prevent the rats from slipping off the runway. The elevated runways prevent the rats from jumping out of the maze. The maze sits within a shielded enclosure (4 m × 5 m) covered by a copper mesh and the mesh is surrounded by white walls in two continuous sides and black curtains in the other two sides. All metal parts are grounded to reduce electrical artifacts during electrophysiological recording.

An Arduino Mega controller was used to receive signals from the shut-off sensors and to send activation signals to the actuators in the treadmills and feeders according to the user-defined sensor and actuator schedule. Custom-made scheduling software by MATLAB was used to monitor the location of the rats via shut-off sensors and to control the actuators in the treadmills and feeders, which enabled the feeders to be turned on and off according to the location of the rat.

Table 2-1 Dimensions of the runway of the reconfigurable maze

Runway type	Combination			
Straight	A, B, C, D, E			
Right	C, F, G, H, I, J, K, L, T			
Left	C, F, G, H, I, J, K, L, T			
Central	C, F, H, I, J, K, L, T			
S-shaped	H, M, N, O, P			
Right and Left	C, Q, R, S, T			
Octagonal field	W, X, T			
Long straight	C, U, V, T			
Basic component	Polygon type	Depth (mm)	Width (mm)	Height (mm)
A	Rectangle	5	490	100
B	Rectangle	5	490	45
C	Rectangle	2	100	5
D	Rectangle	5	100	5
E	Rectangle	5	440	10
F	Non-regular	5	485	100
G	Rectangle	5	485	45
H	Rectangle	5	100	45
I	Rectangle	5	260	45
J	Rectangle	10	480	15
K	Non-regular	10	480	15
L	Non-regular	2	230	10
M	Non-regular	5	480	100
N	Rectangle	5	305	45
O	Non-regular	10	480	15
P	Non-regular	2	180	10
Q	Non-regular	5	490	100
R	Non-regular	2	330	10
S	Non-regular	10	450	15
T	Rectangle	5	100	10
U	Rectangle	5	685	100
V	Rectangle	5	100	10

2.2. Animals

Ten Long–Evans rats purchased from Shimizu Laboratory Supplies, Co. Ltd. (Kyoto, Japan)

were housed individually in cages (20 × 25 × 23 cm) where the light was maintained on a 12-hour light/12-hour dark schedule, with the light phase starting at 8:00 am. The tests were performed during the light phase. The weights of all rats were maintained at 80% of their free-feeding body weight. To examine hippocampal place coding in the maze, a custom-made microdrive was implanted into the dorsal hippocampal CA1 regions of both hemispheres (eight tetrodes each) of four rats to record multiple single-unit activities. All procedures were approved by the Doshisha University Institutional Animal Care and Use Committees.

2.3. Surgery, electrode preparation, and recording

Under isoflurane anesthesia, a custom-made microdrive with 16 independently movable tetrodes was fixed to the skull above the hippocampus of both hemispheres (eight tetrodes each; AP 3.8 mm, ML 3.0 mm, DV 0.5–1.0 mm) of four rats (Table 2-2). After surgery, the electrodes were individually lowered into the pyramidal cell layer of the dorsal hippocampal CA1 region. Extracellular signals were amplified, buffered, digitized, and continuously sampled at 25 kHz using two 32-channel RHD2000 chips (Intan Technologies, Inc., CA) via a motorized commutator (AlphaComm-I; AlphaOmega Inc., Israel). The spikes and local field potential (LFP) were digitally filtered at 800–7.5 kHz and 0.1–200 Hz, respectively. The occurrence of sharp-wave ripple events in the LFP during immobility periods was used to estimate the pyramidal cell layer. After spike sorting using KlustaKwik, putative principal cells were distinguished from fast-spiking cells based on the average firing rate (5 Hz). We defined place cells if the following

criteria were met: the overall firing rate was > 0.1 Hz, spatial information was > 0.1 bit/spike, and maximum firing rate was > 1.0 Hz.

Table 2-2 Variability between rats: electrophysiological measurements

RAT #	ζA	δB	δA	ϵA	Total
No. of pyramidal cells	89	40	46	35	210
No. of interneurons	8	4	9	5	26
Analyses for the square-shaped maze for gap effects					
No. of place cells (spatial information > 0.1 bit/spike & peak firing rate > 1 Hz)	28	18	14	2	62
Spatial information (bits/spike, mean \pm sem)	0.41 \pm 0.05	0.30 \pm 0.03	0.66 \pm 0.13	0.22 \pm 0.06	
Unit isolation quality (isolation distance, Median \pm QD)	8.3 \pm 5.5	5.9 \pm 12.2	14.1 \pm 8.7	6.4 \pm 2.7	
Analyses for the maze morphing from square to cruciform to square					
No. of place cells (spatial information > 0.1 bit/spike & peak firing rate > 1 Hz in any of three situations)	60	24	28	17	129
Spatial information (bits/spike, mean \pm sem)	0.67 \pm 0.11	0.24 \pm 0.03	1.06 \pm 0.17	0.96 \pm 0.34	
Unit isolation quality (isolation distance, Median \pm QD)	8.3 \pm 5.6	6.7 \pm 6.2	6.9 \pm 8.0	6.8 \pm 3.6	

(*) The number of cells meeting the criteria had a large difference between the two conditions because some cells met the criteria either in the square-shaped maze or in the cruciform maze during morphing.

2.4. Behavioral training

All rats were food-restricted and reduced to 80% of their *ad libitum* body weight over a two-week period before training. During this time, they were handled daily. To train the rats to obtain pellets from the food dispenser, they were initially placed in a box (48 cm \times 24 cm, 32 cm height)

with the food dispenser at a corner.

The rats were trained on L-, C-, or G-shaped mazes configured by the reconfigurable maze system in the testing enclosure where they had been habituated to the sounds made by the movable walls being raised and lowered. The rats performed a task in a small, square-shaped maze (overall: 120 cm × 49 cm) in which they ran in a clockwise direction to obtain a pellet. The training lasted until the rat learned to obtain at least one pellet per minute within a 25-minute experimental period. Next, the rats were trained to run in a clockwise direction in a large square-shaped maze (overall: 170 cm × 148 cm) to obtain pellets from two food dispensers located on the left and right sides of the maze. The training lasted for at least 25 minutes per day and continued until the criterion of at least one trial per minute was achieved over one week. After the initial training, the rats were trained to perform the morphing experiment and the spatial alternation tasks described below.

2.5. Morphing experiment

Four rats were trained to run in a clockwise direction on the maze, morphing from square to cruciform to square. They ran for ~1 h in the following sequence: square maze, cruciform maze, and square maze. The 15-minute-long sequences were spaced at ~5-minute intervals, and the rats were rewarded each time they arrived at the food dispensers located on both the left and right sides of the maze. Each maze was morphed within approximately five minutes. The unit recording was performed after the rats had experienced maze morphing over a few days.

2.6. Spatial alternation task

Five rats were trained to alternate between the left and right at a decision point on the figure-8 shaped maze until they achieved an 85% correct rating within 25 minutes. Subsequently, a delay period was incorporated. During the delay period, the rats were locked between two movable walls in front of and behind a treadmill. The treadmill was rotated at a constant speed (~20 m/min) during the delay period. The delay period was increased from 1 s to 7 s every testing day.

2.7. Animal trajectory and head direction

The tips and roots of each rat head were tracked from images captured at 50 or 100 frames per second using a USB3.0 digital video camera mounted on the ceiling of the enclosure using DeepLabCut (Mathis *et al.*, 2018). Initially, 200 annotated images were used to train the pre-trained ResNet-50 network using transfer learning. A few additional iterations of training were then performed with the goal that all Euclidean distances between tracked locations in adjacent frames would be under 50 pixels. The running trajectory was reconstructed by concatenating the tracked roots of the heads. The head directions were computed from the tips and roots of the heads using the inverse of the tangent function.

2.8. Behavioral and neural analyses

The trajectory of the rat was linearized for each trial by projecting the actual trajectory onto a predefined idealized trajectory using nearest-neighbor Delaunay triangulation. The spatial bins

had a resolution of approximately 3 cm.

Rate map: A firing rate map of well-isolated neurons was constructed in a standard manner by dividing the total number of spikes in a bin (3 cm × 3 cm) at a given location by the total amount of time that the rat had been in that bin. Each value was smoothed using a Gaussian filter with a variance of three.

MUA: MUA was calculated by summing the firing of all monitored cells, including low-firing cells and fast-spiking cells.

Spatial information: The spatial information (bits per spike) was used to measure the amount of information a spike conveys about the rat's location on the maze (Skaggs *et al.*, 1992). This was calculated using the following formula.

$$\text{Spatial information} = \sum_i P_i \left(\frac{R_i}{R} \right) \log_2 \left(\frac{R_i}{R} \right)$$

i indexes the position bins, P_i is the probability that the rat was in bin i , R_i is the mean firing rate in bin i , and R is the overall mean firing rate. Based on spatial information, we identified the place cells.

Spatial and rate similarity measures: Spatial similarity is expressed by calculating the spatial correlation of the place fields between the spatially overlapping paths of the square and cruciform mazes. The similarity in firing rates was determined by calculating the difference/sum scores (Leutgeb *et al.*, 2005). The unsigned difference between the two maximum firing frequencies was calculated, and the difference was divided by the sum of the two rates to obtain the score for a set of conditions during maze morphing. Both similarities were expressed using

the cumulative distribution function, $f(X < x)$, which gives the probability that the variable X will be $X < x$ for each real number x .

Bayesian decoding: A memoryless Bayesian decoder (Zhang *et al.*, 1998) was used to decode the rat's locations based on place cell activity. First, the probability of a rat's location based on place cell firing within a time window was estimated as follows.

$$\text{Prob}(Pos | spikes) = \left(\prod_{i=1}^N f_i(Pos)^{n_i} \right) \exp^{-\tau \sum_{i=1}^N f_i(Pos)}$$

f_i and n_i represent the place map and the number of spikes of the i -th place cell within the time window, respectively. N indicates the total number of place cells, and τ represents the duration of the time window.

The probability within each time window was normalized for every location as follows (Pfeiffer and Foster, 2013).

$$\text{nProb}(Pos | spikes) = \frac{\text{Prob}(Pos_k | spikes)}{\sum_{k=1}^M \text{Prob}(Pos_k | spikes)}$$

$\text{Prob}(Pos_k | spikes)$ represents the probability at the k -th location bin within the time window, and M represents the total number of location bins.

The time window was set at 300 ms. A point estimation of the location was made using a maximum likelihood estimation.

2.9. Statistical analyses

Analyses of rat behavior around the gaps: Any running speed or head direction values that exceeded more than three times the local scaled median absolute deviation (MAD) away from the local median within a sliding window (~72 cm) were defined as outliers. The two-tailed Wilcoxon rank-sum test was used to assess the gap effect on rats' behaviors in terms of running speed and head direction (Figure 3-6). Differences in the running speed and head direction between gap locations between runways and the corresponding locations on the long gapless runway were assessed using the two-way repeated-measures analysis of variance (ANOVA) (Figure 3-7). Differences in occupancy time at gap locations were assessed using the one-way repeated-measures ANOVA (Figure 3-8). The occupancy time was calculated as the duration that the rat occupied the gap location. The durations where the rat paused (running speed < 5 cm/s) were excluded from the analysis.

Analyses of neural activity around gaps: To examine whether the width of the place field was specifically changed at the gap locations, the Monte Carlo method was used. For each cell, the original place field location was shifted by a pseudo-random interval between 20 bins and 20 bins less than the length of the entire linearized track, with the end of the track wrapped at the beginning. This procedure was repeated 3,000 times for each cell. For each shuffling, the width of the place field, which is defined as the length of the firing field whose firing rate is over one-third of its maximum firing rate, was calculated. Whether the place field on the gaps had a width greater than the 5th percentile or lower than the 95th percentile of the shuffled data was determined (Figure 3-9 B). The two-tailed Wilcoxon rank-sum test was used to assess the

number of place fields, firing rates of MUA, and Bayesian decoding errors of the gap locations compared to the non-gap locations (Figures 3-10 and 3-11 B).

Analysis of learning performance: The differences in learning curves were assessed using one-way repeated-measures analysis of variance (Figures 3-12 B and D). A two-way mixed ANOVA was used to ascertain the effect of expertise and experience on assembly time and their potential interaction (Figure 3-3). Differences in spatial and rate similarities were assessed using the two-tailed Wilcoxon signed-rank test (Figure 3-15).

All analyses were performed using custom-made programs based on MATLAB functions (v9.6; MathWorks, Natick, MA).

2.10. Histology

To identify the final recording locations, four rats were deeply anesthetized with isoflurane (Pfizer Japan Inc., Tokyo, Japan) and then administered an overdose of pentobarbital sodium salt (50 mg/kg, intraperitoneal [i.p.]; Nacalai Tesque Inc., Kyoto, Japan) and transcardially perfused with phosphate-buffered saline (PBS), followed by 10% phosphate-buffered formalin fixative (3.5-3.8% formaldehyde). Their brains were cut coronally at 40 μm and stained with cresyl violet. The final location of the tip of each electrode was around or below the pyramidal cell layer of the dorsal hippocampal CA1 region.

3. Results

3.1. Implementation of the reconfigurable maze

We developed a maze system that enables the shape of the maze to be reconfigured in a single physical environment using interlocking runways. Figure 3-1 demonstrates the existing standard mazes configured by our maze system in an enclosure, namely, the T-maze, W-maze, figure-8 maze, plus maze, and radial arm maze.

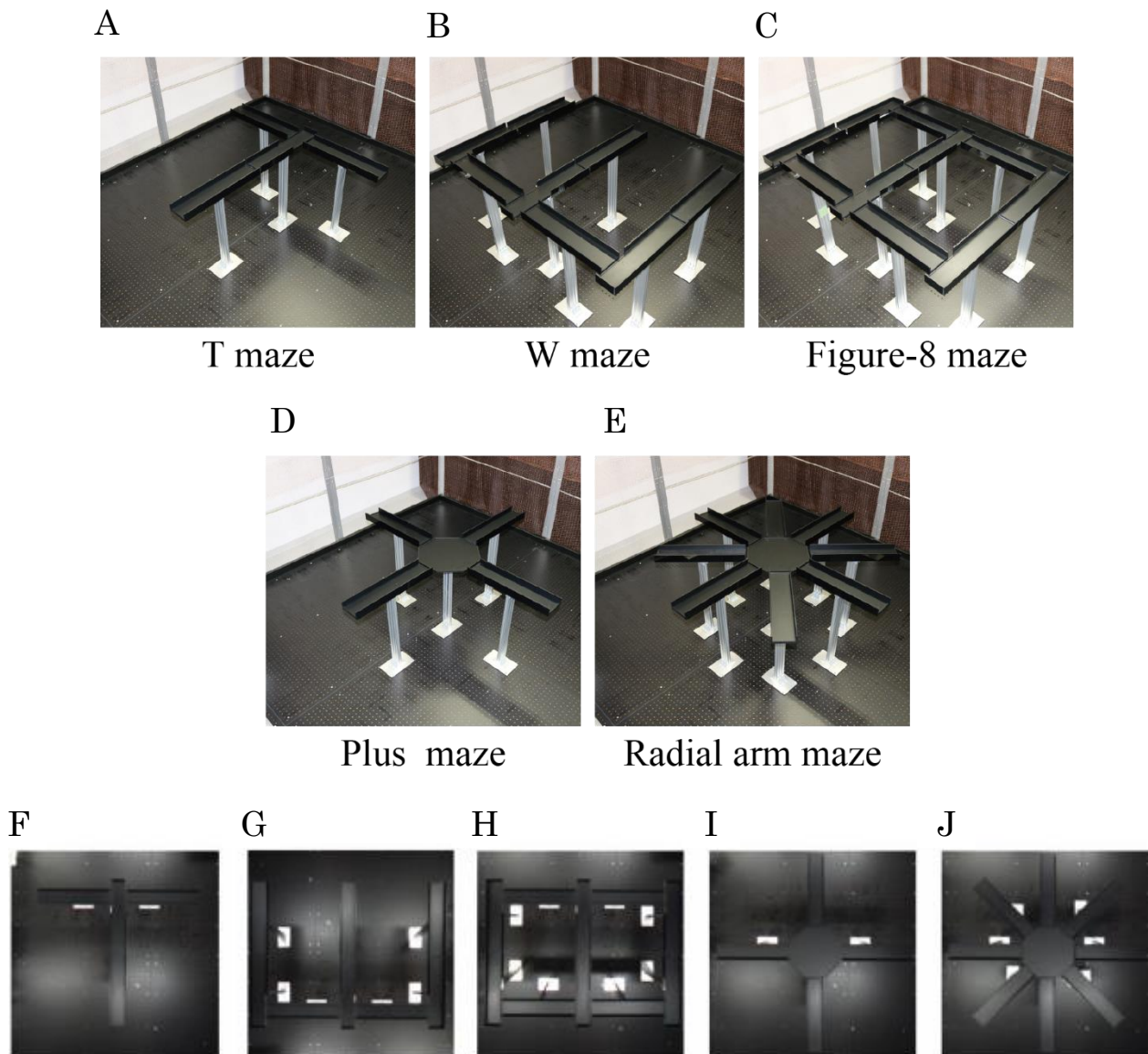


Figure 3-1 Maze reproduced by the Reconfigurable Maze

(A-E) The maze can be configured to form T (A), W (B), figure-8 (C), plus (D), and radial arm (E) mazes in a single enclosure.

(F-J) The top view of T (F), W (G), figure-8 (H), plus (I), and radial arm (J) mazes.

Each runway was placed atop towers with baseplates (Figure 3-2 A). These baseplates have protrusions that connect to a grid of holes in a floor-based breadboard (Figure 3-2B). The insertion of the protrusions into the holes of breadboard enables coordination with the grid pattern and minimizes swinging of the runways resulting from the movement of the animal. Similarly, an array of accompanying parts, including feeders, movable walls, and treadmills placed atop towers on their own can also be attached to the breadboards. Thus, the feeder can be placed on the side of any runway to change the reward location (Figure 3-2 C). The movable wall can be placed at any of the interlocking gaps between runways as a dead end to dynamically control possible running paths (Figure 3-2 D), and any runway can be replaced by a treadmill (Figure 3-2 E). Moreover, the shut-off sensor can be attached alongside any runway to signal a triggering event to the feeders and treadmills (Figure 3-2 F, arrows). Placing these interlocking parts onto the grid pattern enables the researchers, even if they are not familiar with the maze, to precisely reproduce a variety of coordinated patterns of mazes for a brief period, in a repeatable manner, in a single physical environment.

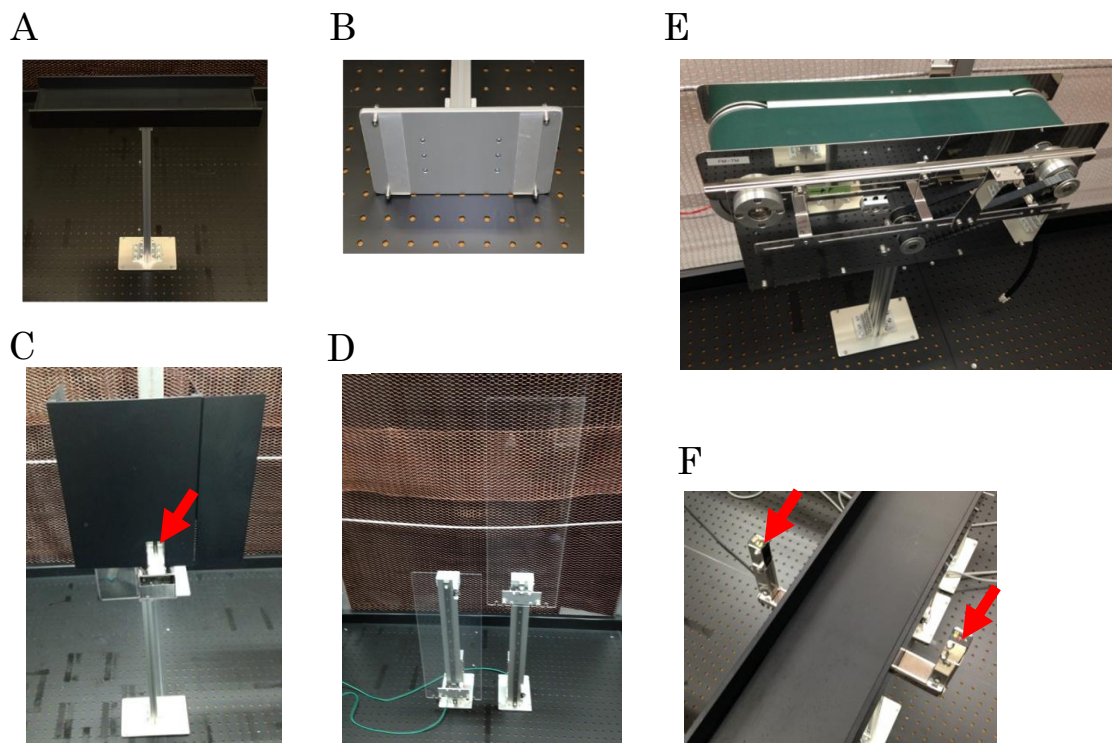


Figure 3-2 Interlocking mechanisms and accompanying parts

(A) Runway sections are placed atop towers.

(B) The baseplate of each tower has four protrusions that coordinate the placement of the section on the breadboard in a flexible, repeatable manner (see also Figure 3-4).

(C-F) An array of accompanying parts. (C) A feeder. Rats acquire pellets by poking into the opening (arrow). (D) Movable walls. The left is lowered state, and the right is raised. (E) A treadmill. (F) A shut-off sensor (arrows).

The maze also provides a scalable experimental setup because the complexity and area of the maze are incrementally expandable by adding extra parts. When the morphing of a maze from square to cruciform was timed, the assembly time for beginners was not significantly different from that for experts who had used the reconfigurable maze daily for 3 months (3 experts: 131 ± 9 s; 3 beginners: 158 ± 12 s [mean \pm SEM]; Figure 3-3). Instead of runways, open platforms can also be embedded into the maze, which enables the plus maze and radial arm maze to be configured (Figure 3-1 D and E). Furthermore, the scheduler for the timing of sensors and actuators installed in the accompanying parts allows the researcher to design several behavioral

tasks, even within a single maze shape. This flexible maze design also allows researchers to rapidly select tasks that best match the needs of a particular experiment during preliminary studies.

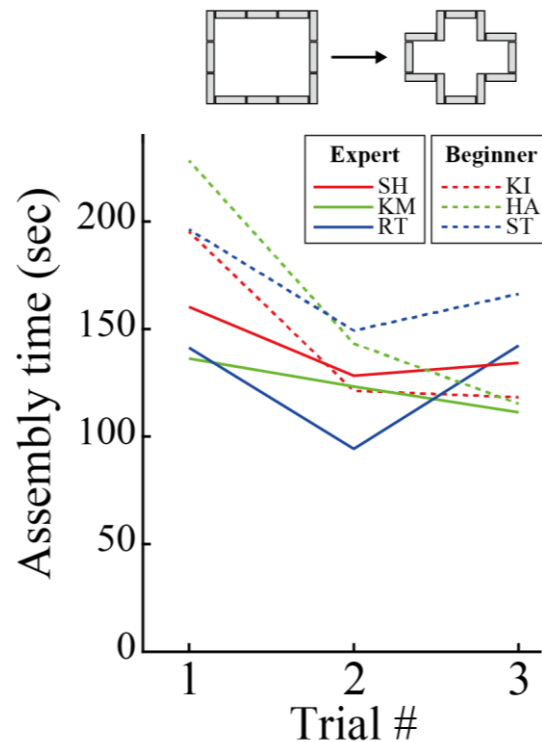


Figure 3-3 Assembly time of the reconfigurable maze for morphing the shape from square to cruciform

Performance improved with consecutive trials in a day (performance versus trial: $F_{2,8} = 7.453$, $p = 0.0149$), but not with expertise (expert/beginner) (performance versus expertise: $F_{1,4} = 5.654$, $p = 0.0762$). There was no significant interaction between expertise and experience in a day (expertise versus trial: $F_{2,8} = 0.320$, $p = 0.735$). Two-way mixed ANOVA was used.

3.2. Interlocking gaps do not alter navigational behavior

To manufacture the interlocking parts at a reasonable cost or by hand, a short gap between runways (~1 cm) (Figure 3-4 A) is a prerequisite margin so that the parts can interlock. Ideally, perfectly manufactured parts with a precision of less than 1 mm would not require these gaps as margins; however, such high-precision manufacturing is expensive and does not permit the use of low-precision handcrafted parts. When the gaps are not included as margins, runways

manufactured with lower precision (> 1 cm) will overlap if the location of the runway is slightly shifted, as shown in Figure 3-4.

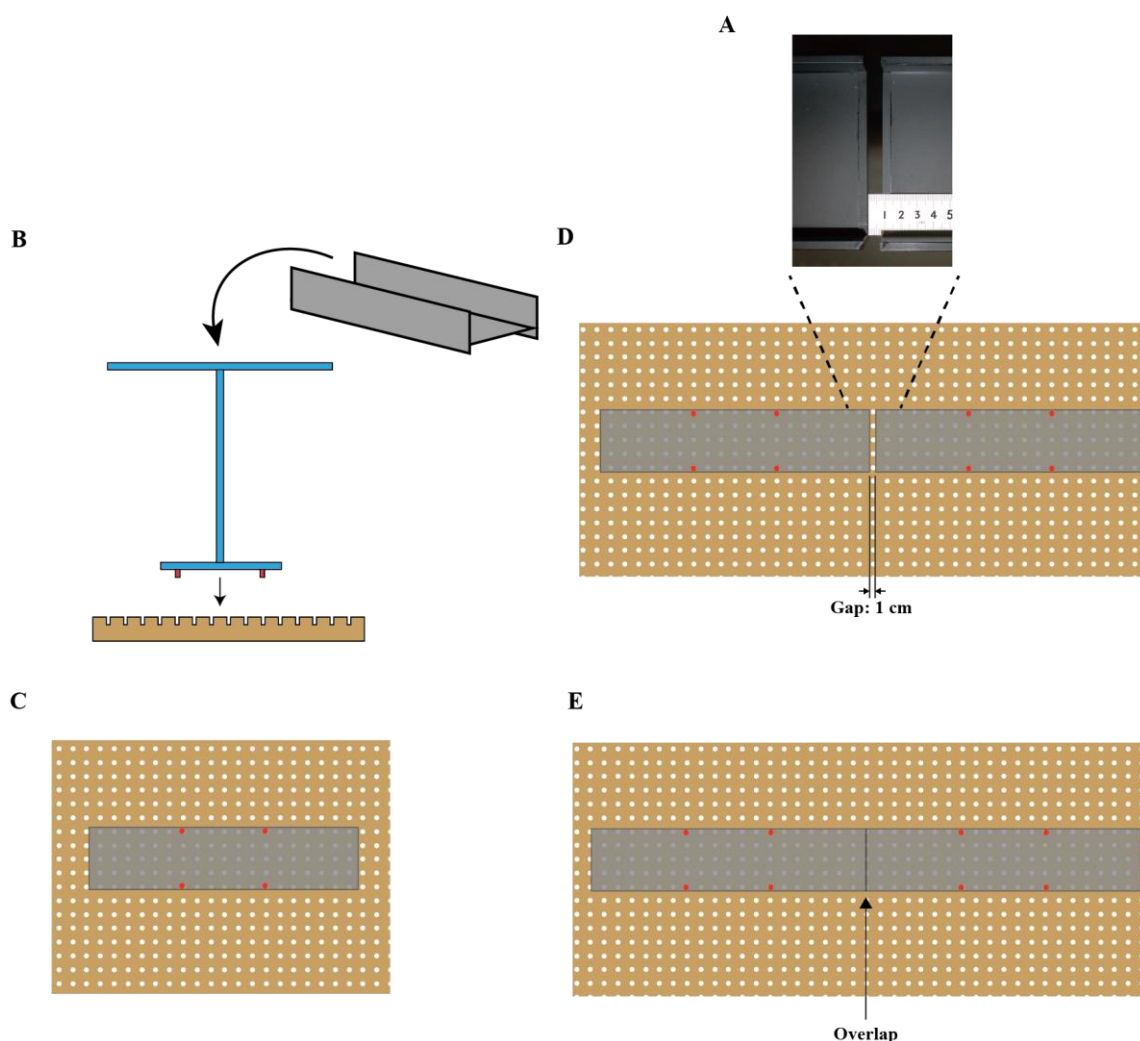


Figure 3-4 A short gap between runways is a prerequisite margin for the interlocking parts.

(A) Close-up photo showing the gap.

(B) The runway (gray) is placed atop a tower (blue) on a breadboard (brown) with a grid of holes. The baseplate of the tower has protrusions (red) that coordinate the placement of the section on the breadboard.

(C) Top view of a runway on the breadboard.

(D) Two runways with a 1-cm gap.

(E) This view demonstrates that the runways overlap only if the total dimensional error exceeds a precision of 1 cm.

We next answered the question of whether this gap affected animal behavior. Four rats were trained to run smoothly along a square-shaped maze in a clockwise direction (Figure 3-5). The

running speed at the gaps did not abruptly change from the running speed between the gaps (Figure 3-6 A). The incidence of abrupt changes in the head direction was significantly lower at the gaps than that between the gaps (Figure 3-6 B). These results suggest that the gaps did not distort the behavior of normal rats.

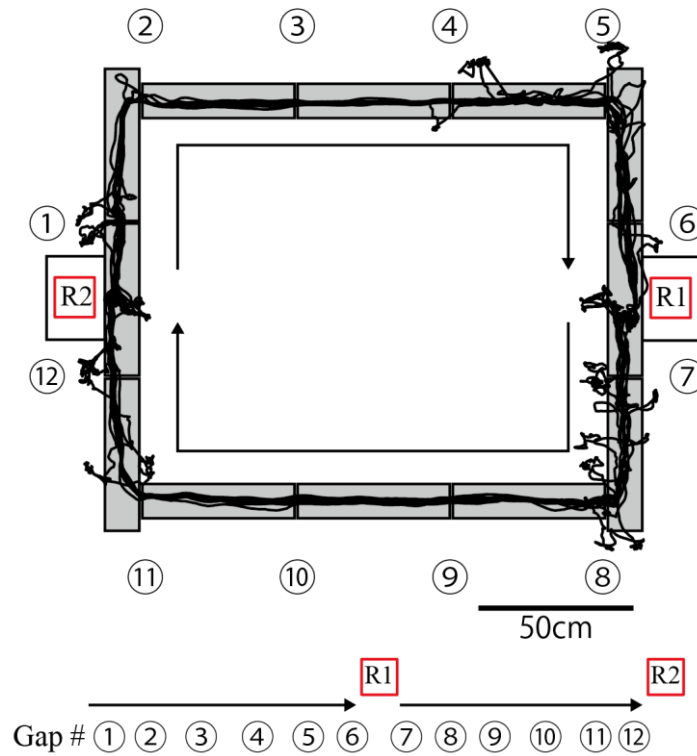


Figure 3-5 Schematics of the square-shaped maze test

An example running trajectory of a rat is superimposed on the maze. The numbers indicate gap locations. R1 and R2 indicate food dispensers. Linearized gap locations are illustrated at the bottom.

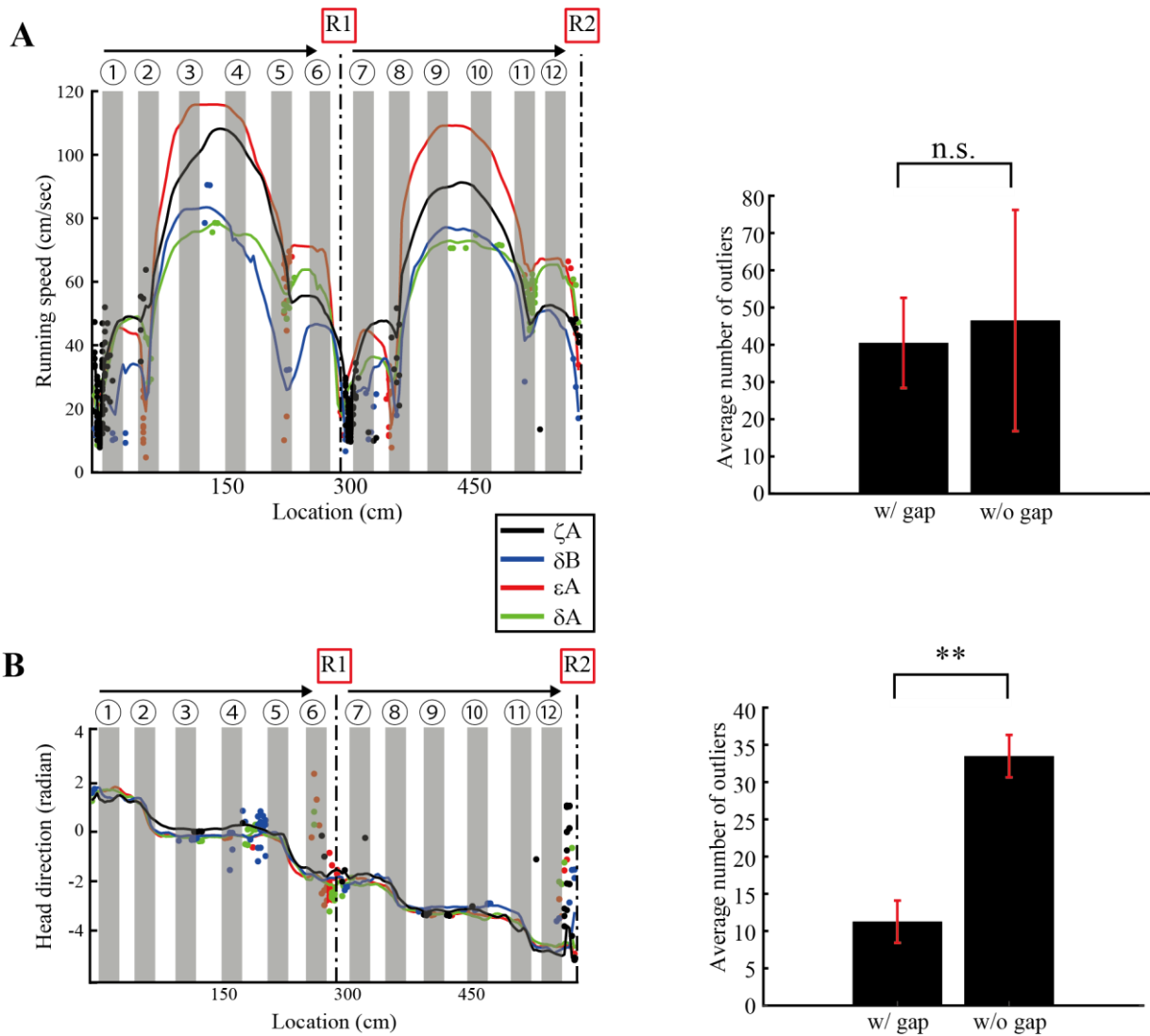


Figure 3-6 Running speed and head direction on the runway with or without gaps (A and B) Left, the average running speed and head direction of four rats as a function of the linearized location. The dots indicate the location of outliers for each lap. Right, the average number of outliers on the regions around the gap (gray shaded areas) and other regions (running speed: $t = -0.19$, $df = 6$, $p = 0.86$; head direction: $t = -5.53$, $df = 6$, $p = 0.0015$, two-tailed paired t -test). $**p < 0.01$, n.s.: $p > 0.05$. Error bars indicate the SEM.

To corroborate the results, we prepared two gapless runways with total lengths (149 cm long) that were the same as those of the three interlocking runways, including the gaps between the sections. We then replaced the three runway sections at the top or bottom of the square-shaped maze with a single runway without gaps (Figure 3-7 A). Five rats were trained to run on the maze, with or without gaps, over a 20-min interval. The running speed and head direction values on the gaps were not significantly different from those on the corresponding portions of the single runway without gaps (Figures 3-7 B and C).

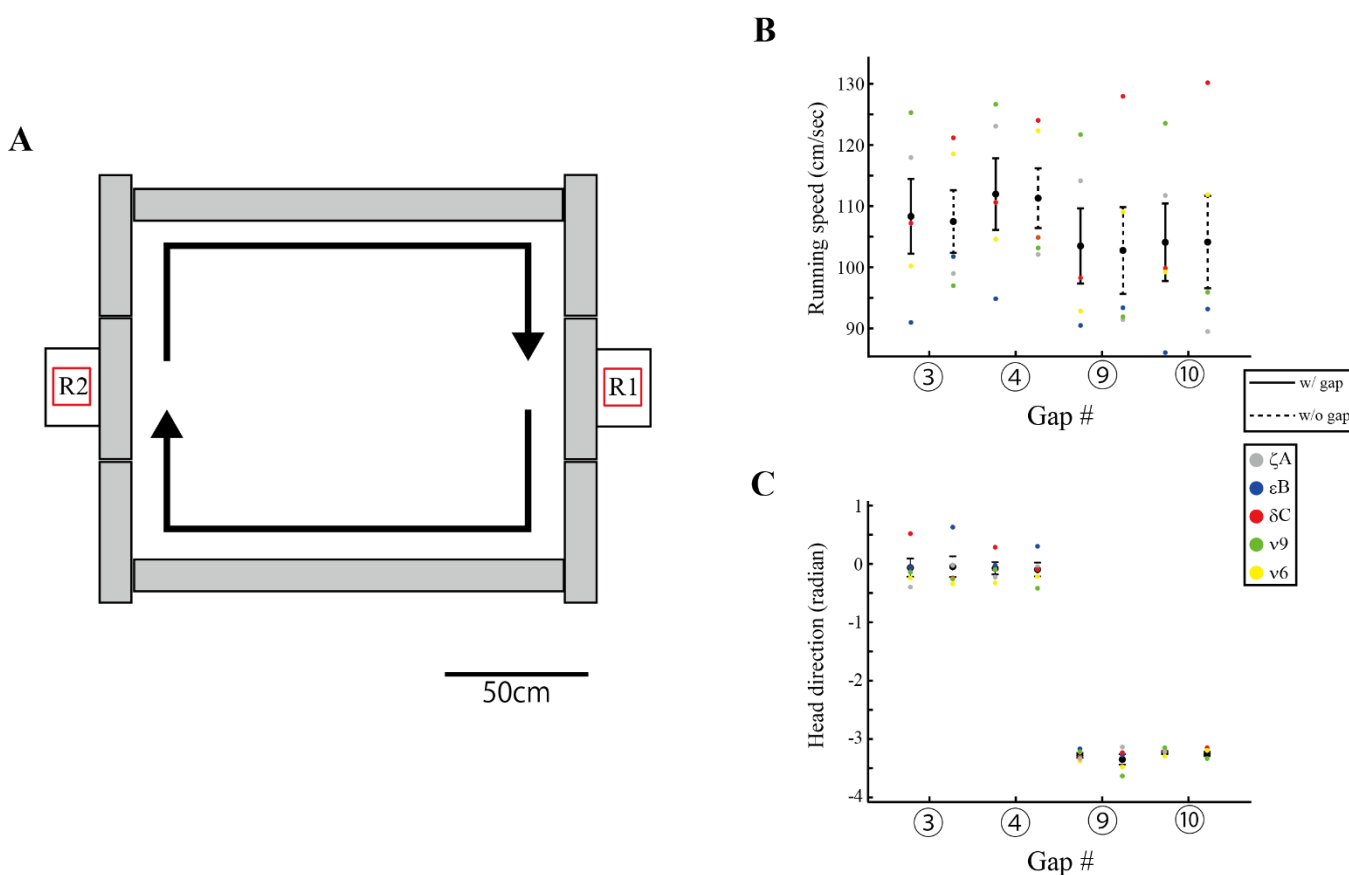


Figure 3-7 Square-shaped maze test with long runways

(A) Schematic showing two gapless runways placed at the top and bottom of the square-shaped maze. R1 and R2 indicate food dispensers. (B–C) The running speed (B) and head direction (C) of five rats on the runways with gaps (solid line) and without gaps (dotted line) as a function of the examined gap locations. The data from individual animals are overlapped as color-coded dots. Neither running speed nor head direction was influenced by the presence of a gap (simple main effect: gap presence *vs.* running speed between all pairs of the examined gaps: $p < 0.05$, gap presence *vs.* head direction between all pairs of the examined gaps: $p < 0.05$). However, there were interactions between gap presence and location (running speed: $F_{1,4} = 2653.9$, $p < 10^{-6}$; head direction: $F_{1,4} = 302.3$, $p < 10^{-4}$) shown using two-way repeated measures ANOVA. Error bars indicate the SEM.

As shown from the trajectory (Figure 3-5) and abrupt changes in the head direction (Figure 3-6 B), the rats frequently decelerated or stopped at preferred locations. Such pausing locations differed from rat to rat and were accompanied by rearing and grooming, which may be related to home base behavior (Eilam and Golani, 1989). To examine whether such pauses are preferentially observed at gap locations, four rats were trained to run in a clockwise direction on a square-shaped maze configuration. All rats paused and exhibited rearing and grooming around the food dispensers and corners. The occupancy time when the rats visited the gap location around a food dispenser (gap #7) was significantly longer than their occupancy times at the other two gaps (gaps #3 and #10) (Figure 3-8), suggesting that unidentified factors, excluding gap presence, might also affect the behavior of the rats around food dispensers or corners. In addition, it is well known that such stopping behaviors modulate the hippocampal neuronal activity (Foster and Wilson, 2006). Thus, to exclusively examine the gap effects, we focused on the gaps (#3, #4, #9, and #10) between the three interlocking runways arranged in a straight line on the top and bottom sides of the square-shaped maze in the subsequent analyses.

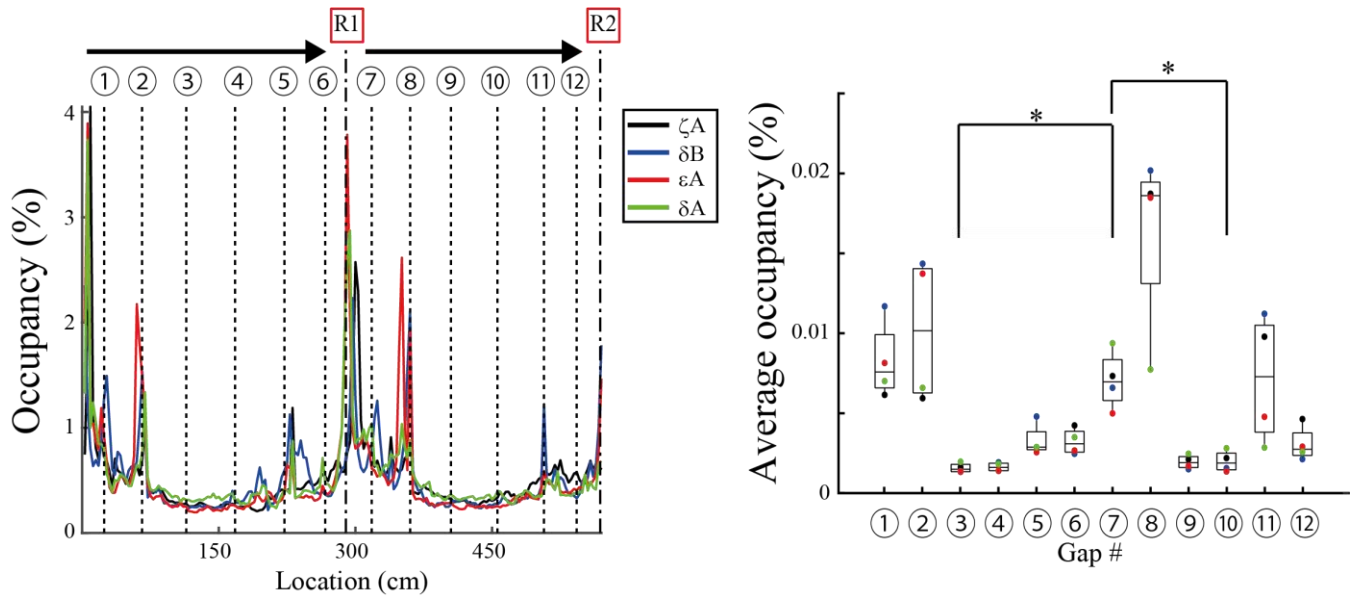


Figure 3-8 Occupancy time over the maze

Left, the percentage of the occupancy time over the entire maze as a function of the linearized location of four rats. Right, the median percentage of the occupancy time at gap locations (medians, first and third quartiles, minimums, and maximums are indicated). The rats preferentially slow down at gap #7 compared to gaps #3 and #10, which are located at the top and bottom of the maze ($F_{1,3} = 152.69$, $p = 0.0011$; gap #7 versus #3: $p = 0.049$; gap #7 versus #10: $p = 0.030$, one-way repeated-measures ANOVA with post hoc Tukey's honestly significant difference test). * $p < 0.05$

3.3. Interlocking gaps do not alter hippocampal place coding

The results in the previous chapter suggest that spatial gaps do not affect the navigation behavior of rats. On the other hand, spatial gaps can serve as visual cues, which may alter the activity of place cells when compared to pathways without gaps (Sharif *et al.*, 2021). To determine whether the gaps distort neuronal activity, we monitored the activity of 236 neurons from the hippocampal CA1 of both hemispheres of four rats running on the square-shaped maze in a clockwise direction (Figure 3-9, Table 2-2). Neuronal recordings were performed after the rats were sufficiently familiarized with the gapped square-shaped maze, and data analysis was mainly focused on gaps 3, 4, 9, and 10 and the pathways between them (Figure 3-9 A). The average width of the place fields of 62 place cells on the gaps settled between the 5th and 95th percentiles of distribution for shuffled data from the entire set of place fields (Figure 3-9 C).

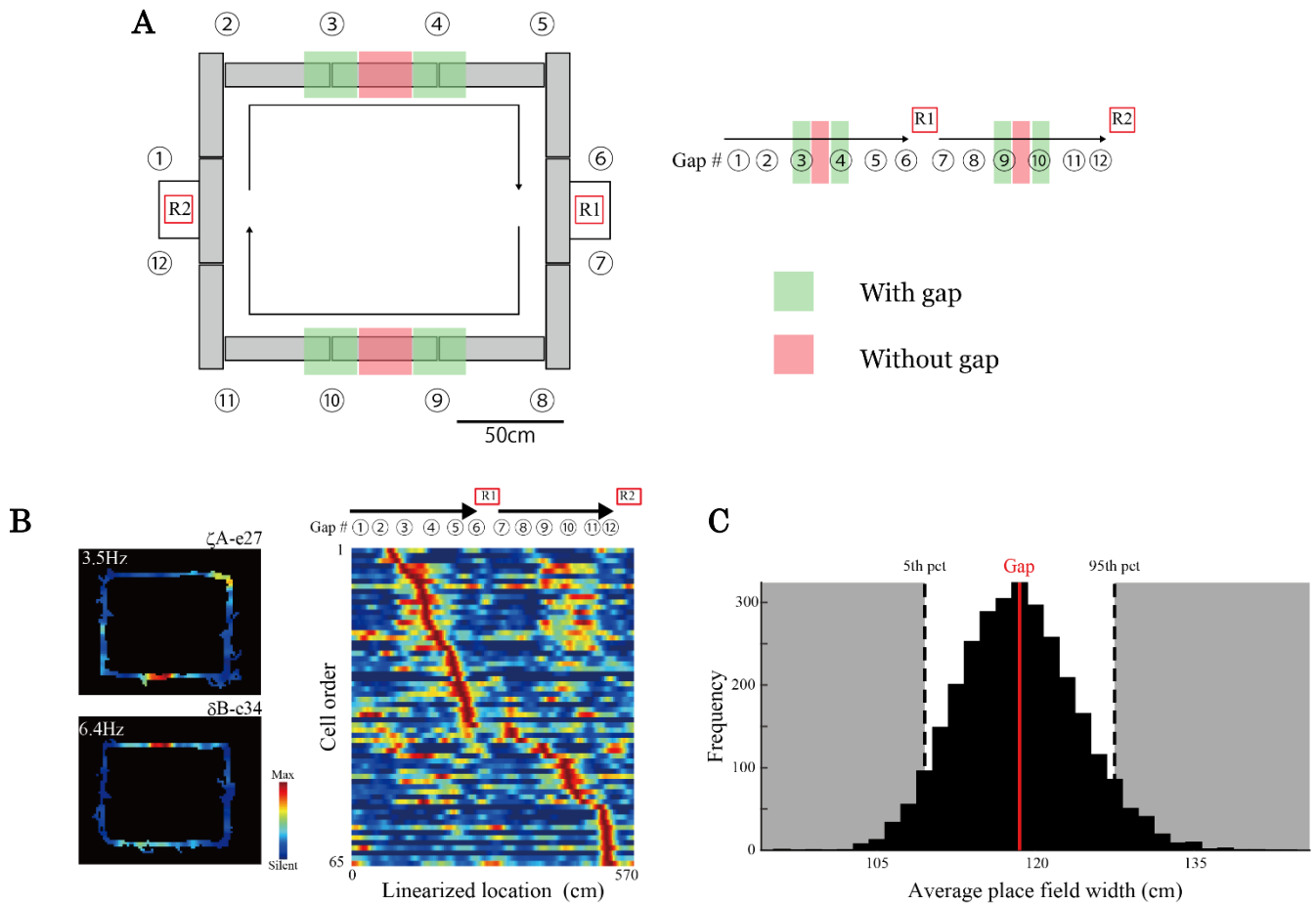


Figure 3-9 Place cells and lengths of the receptive fields

(A) Left, schematic diagrams of square-shaped maze test. The numbers indicate gap locations. R1 and R2 indicate food dispensers. Right, linearized locations of gaps and rewards. The analysis focused on gaps 3, 4, 9, and 10 (green meshes) and the runways between them (magenta meshes).

(B) Left, normalized firing rate map of two representative place cells that have place fields around gap locations in the hippocampal CA1 region on the square-shaped maze configuration. Right, normalized firing rate maps of 65 hippocampal place cells simultaneously monitored from a rat (ζ A) ordered by the latency of their peak firing rates. Each line is a single unit. Gap locations are indicated at the top. Red indicates maximum firing rates, and blue indicates silent.

(C) Distribution of the average width of place fields randomly shuffled from the original sample covering the gaps (3,000 shuffles). The red line indicates the average width of the place fields on the gaps. Dotted lines indicate the 5th and 95th percentiles for the shuffled data.

Moreover, on the gaps, the number of place fields from the 62 place cells and the firing rate of multiunit activity in the hippocampal CA1 region did not change in comparison to the recordings taken between the gaps (Figures 3-10 A and B). At the ensemble level, the trajectory decoded from the activity of simultaneously monitored place cells using a memoryless Bayesian decoder

(Zhang *et al.*, 1998) depicted a seamless path, even at the gap locations (Figure 3-11). Thus, both behavioral and neuronal responses at the gaps support the view that rats behave as if they perceive the interlocking gap and gapless portions on the runways similarly.

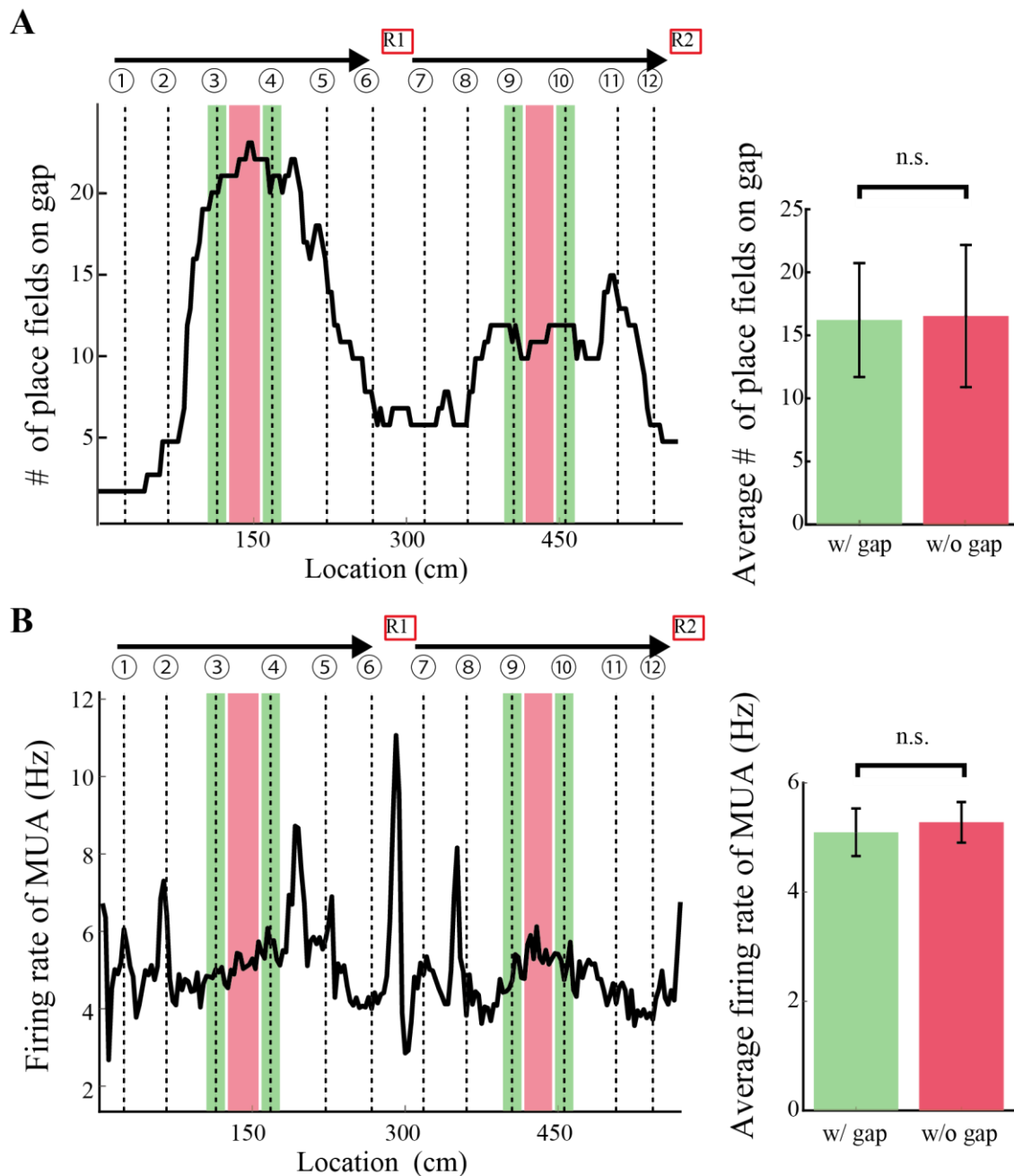


Figure 3-10 Number of place fields and firing rate of multiunit activity

(A and B) Left, the number of place fields (A) and the firing rate of multiunit activity (MUA) in the hippocampal CA1 region (B) as a function of linearized location on the square-shaped maze. Right, the average number of place fields (A) ($z = 0.14$, $p = 0.89$) and the average firing rate of MUA ($z = -1.51$, $p = 0.13$) on the gaps (#3, 4, 9, 10) (green shaded area) and between them (orange shaded area).

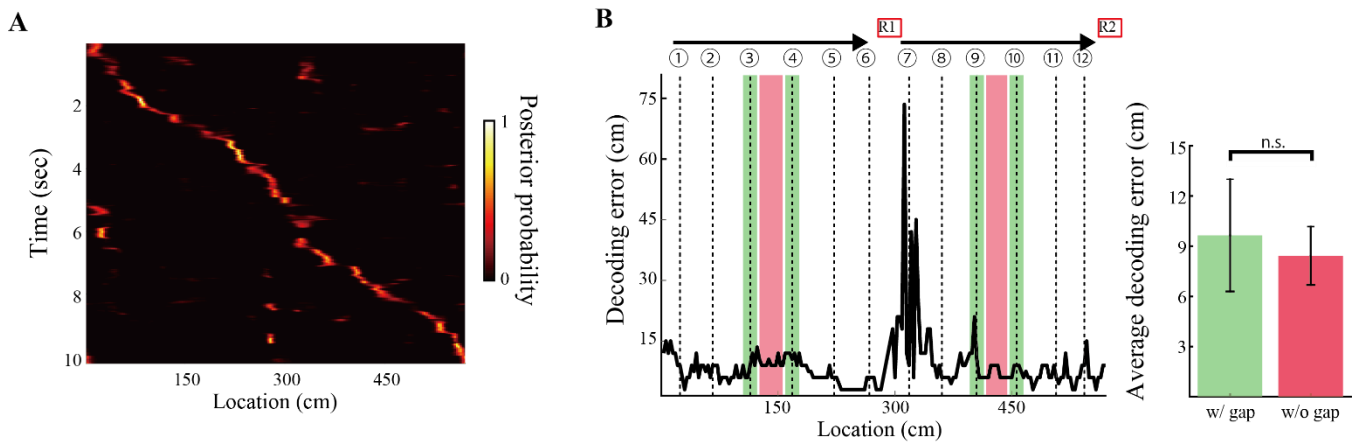


Figure 3-11 Estimation of the rats' position

(A) Representative posterior probability of locations decoded by the Bayesian decoder from 89 simultaneously monitored cells. Values are indicated by the color bar (right).

(B) Left, the difference between the actual and decoded locations as a function of linearized location on the square-shaped maze. Right, the average difference between actual and decoded locations on the gaps (#3, 4, 9, 10) (green shaded area) and between them (orange shaded area) ($z = 1.34$, $p = 0.18$). The bin width was set at 3 cm.

3.4. Rats can learn spatial alternation tasks in the reconfigured maze

Spatial alternation tasks are often used to detect hippocampal lesions (Deacon and Rawlins, 2006). In this study, we investigated whether the reconfigurable maze system can train rats such alternation tasks. After the five rats became familiar with the square-shaped maze, the maze was morphed from the square to the figure-8 shape using the reconfigurable maze system. The rats were trained to alternate between the left and right branches of the central stem for 1 h per day over 5 days (Figure 3-12 A). All rats gradually learned the spatial alternation task (Figure 3-12 C). They achieved a mean score of greater than 80% correct choices over 50 consecutive trials on the second day. To demonstrate the usability of the attachable walls and treadmills, three rats were tested on a delayed version of the spatial alternation task by partially reconfiguring the maze: a runway in the center of the stem in the figure-8-shaped maze was replaced by a treadmill

(Figure 3-12 B). To force the rats to run on the treadmill for a 7-s delay period, movable walls were set at the gaps in front and behind the treadmill. The rats achieved a mean score of greater than 70% correct choices over 50 consecutive trials at the beginning, and their performance improved after 10 days of testing (Figure 3-12 D). The results suggest that the reconfigurable maze system can be used to train rats to perform normal and delayed spatial alternation tasks.

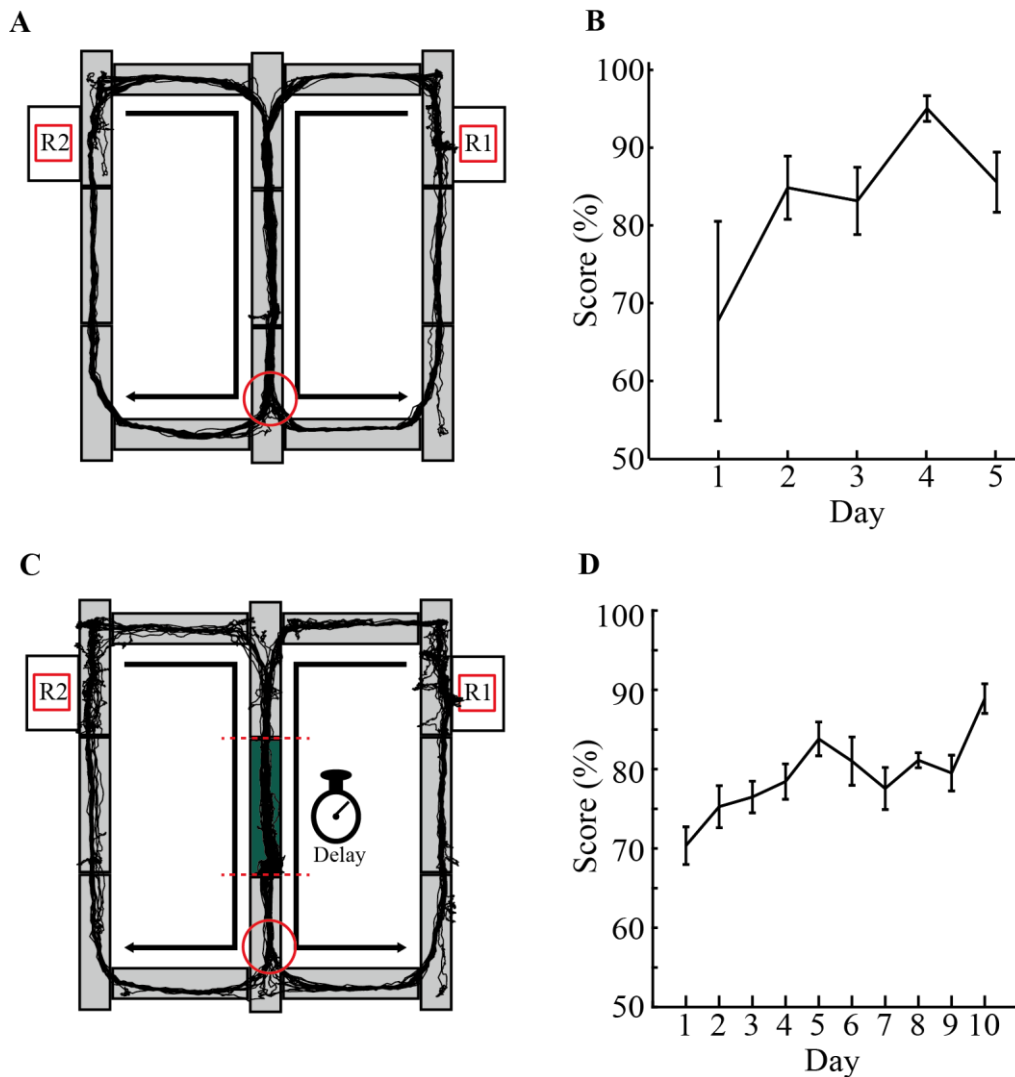


Figure 3-12 Learning of the spatial alternation tasks

(A) Schematic representation of the figure-8-shaped maze created using the reconfigurable maze. Example animal trajectories are superimposed on top of the maze. The red circle indicates a branch point where the rat must decide which direction to turn.

(B) Spatial alternation task performance improved with experience (performance versus testing day: $F_{1,4} = 795.9, p < 10^{-5}$).

(C) Same as in (A) but with a treadmill (green). Red dashed lines indicate the gap locations where movable walls are placed to force the rats to run on the treadmill for a delayed period.

(D) Performance of the delayed version of the spatial alternation task of rats improved with experience (performance versus testing day: $F_{1,2} = 531.8, p = 0.0019$). All results are from the one-way repeated-measures ANOVA. Error bars indicate the SEM.

3.5. Place field remapping during the maze morphing experiment

Several lines of evidence suggest that hippocampal place coding partially or completely changes in response to proximal or distal cues (Muller and Kubie, 1987; Leutgeb *et al.*, 2005). This phenomenon is called remapping of place fields. Since the reconfigurable maze system can deform a part of the maze shape while keeping other conditions fixed, it may enable us to perform experiments that are not possible with existing mazes that could not be easily deformed. To demonstrate the ability to transform a maze while keeping its scale, proximal, and distal cues the same, we provide a novel morphing experiment to examine the remapping of place fields between different shapes of a maze. This maze maintains an identical path length when the maze shape morphs from square to cruciform to square. As the cruciform maze is an internal structure of the square maze, the total path length does not change during morphing. Moreover, the four outermost runways of the cruciform maze physically overlapped with the path of the square-shaped maze (Figure 3-13). As our maze provides morphing in one enclosure, it enables the identification of factors influencing hippocampal place coding: path integration and spatial reference frame.

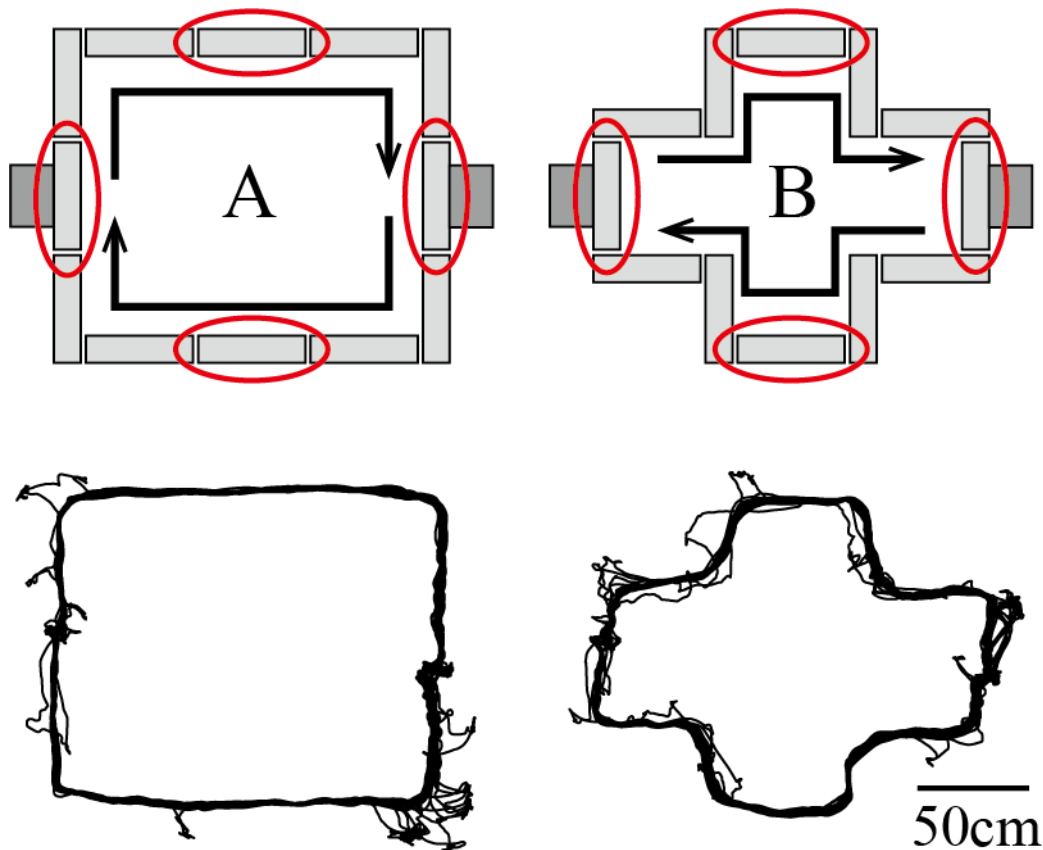


Figure 3-13 Maze morphing experiment

Schematics of the square and cruciform mazes configured by our system (top) and the representative running trajectory of a rat (bottom). The runways enclosed by red circles were not moved during the morphing experiment.

To examine the remapping of the place fields, we examined 129 place cells monitored from the dorsal hippocampal CA1 regions of four rats. In the experiment, the maze transformed from a square to a cruciform shape and back to a square again. The animals were exposed to each maze for 15 minutes and three rate maps were calculated for each place cell (Figure 3-14). The total path length of the runway and available distal cues in the maze were nearly identical across the maze shape morphs. In contrast, between the first and second exposures, the spatial correlation of the firing rate map of the place cells that were within the overlapping runways in the square-shaped maze was significantly larger than that between the square-shaped maze and the cruciform maze (Figures 3-14 and 3-15 A). This suggests that the maze shape can be a cue capable

of inducing remapping of the location of place fields as a spatial reference frame. Moreover, between the first and second exposures, the difference in the maximum firing rate of place fields within the overlapping runways in the square-shaped maze was similar to that between the square-shaped maze and the cruciform maze (Figures 3-14 and 3-15 B). These results suggest that maze morphing from square to cruciform is represented by a difference in the place field locations without a change in the place field firing rate.

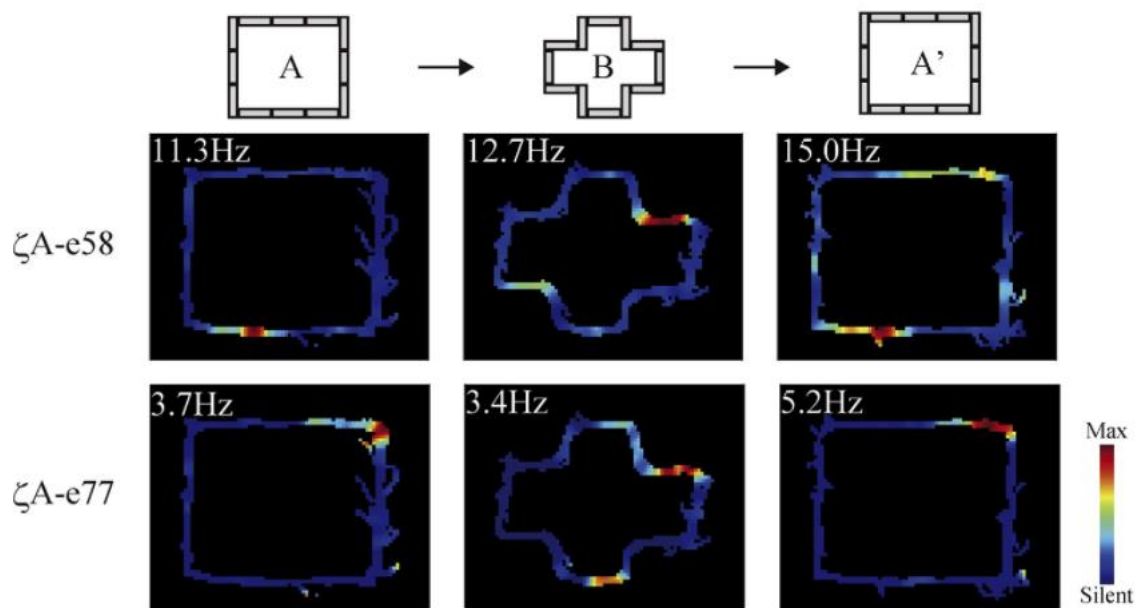


Figure 3-14 Place cells in the morphing experiment

Representative change of the place field of a place cell recorded from a rat (ζA) during maze morphing. The maximum firing rate is displayed in the top left corner.

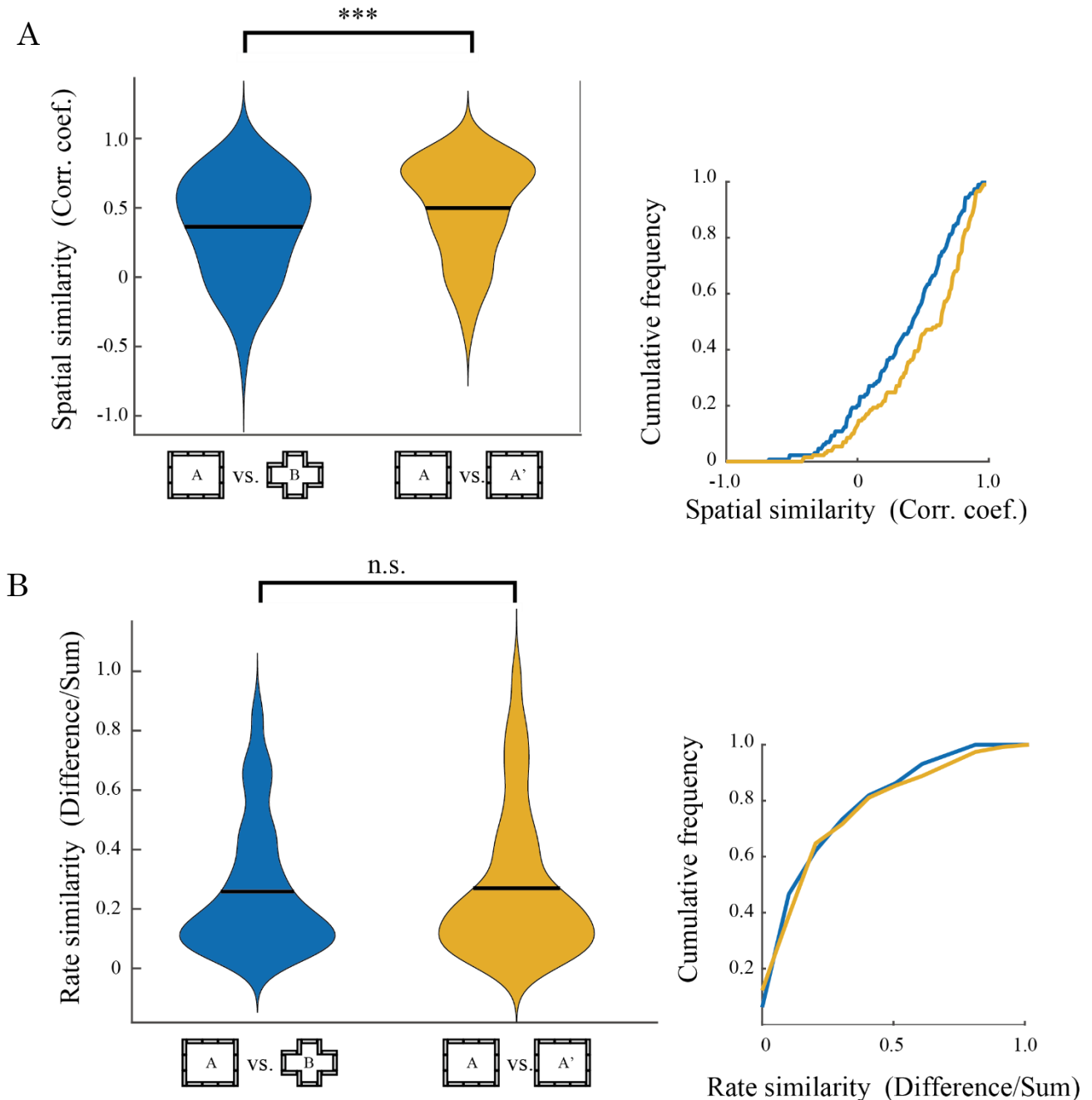


Figure 3-15 Spatial similarity and rate similarity

(A and B) Violin plots with spatial similarity demonstrated as the spatial correlation of the firing rate map (A) ($z = -3.98$, $p = 10^{-4}$) and the rate similarity as the firing rate difference within place fields (B) ($z = -0.60$, $p = 0.55$) between the square maze and cruciform maze as well as between the first and second exposures of the square maze (left). Black bars indicate the median values. Surrounding each side is a rotated kernel density plot. Their cumulative frequency is graphed to the right. All values were acquired from the two-tailed Wilcoxon signed-rank test. *** $p < 0.001$, n.s.: $p > 0.05$.

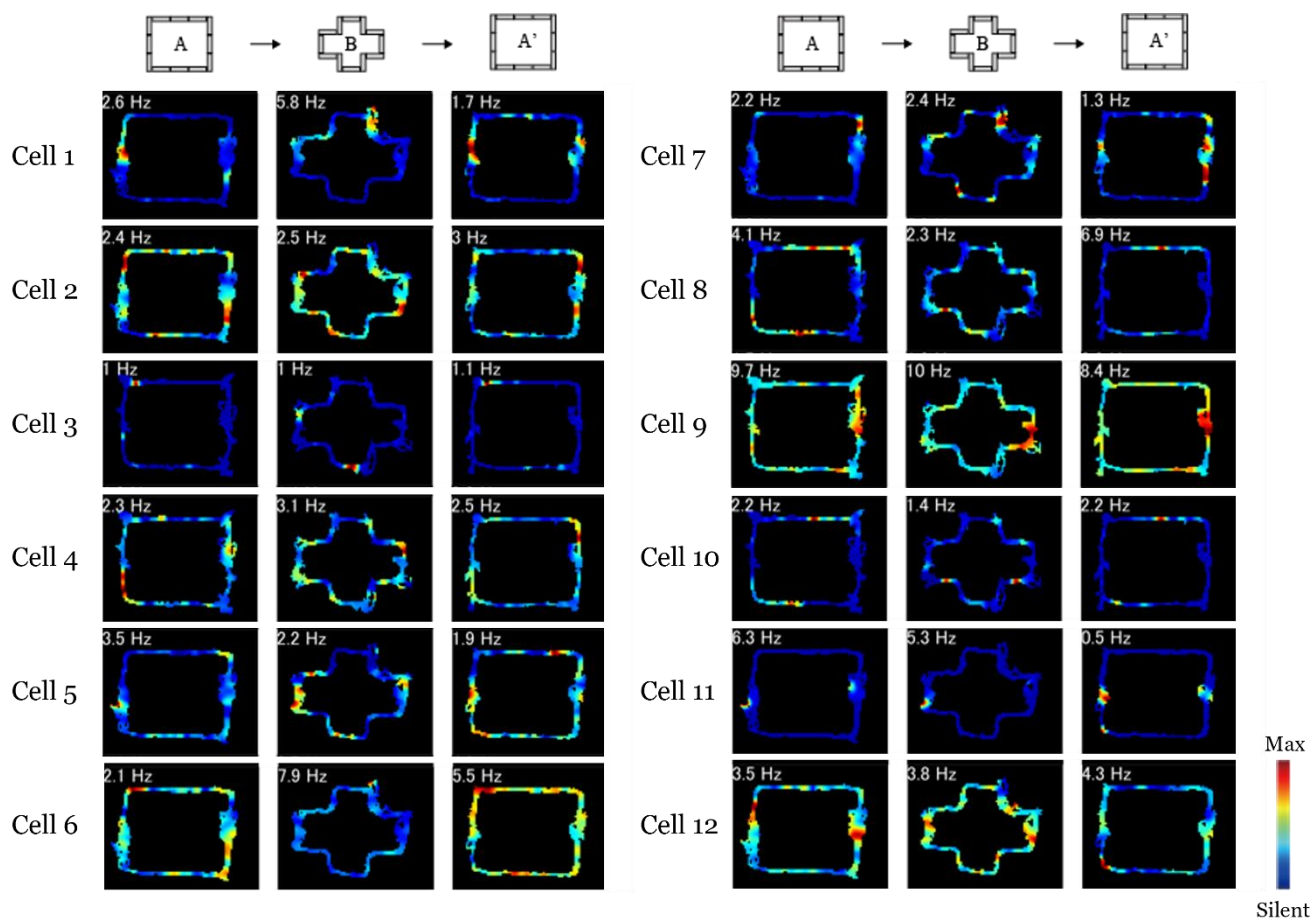


Figure 3-16 More examples of place cells

The view of the figures is the same as figure 3 -14. See also table 2-1 for place cell properties.

4. Discussion

In this study, we developed a reconfigurable maze consisting of a series of systems that can transform the shape of a pathway to reproduce spatial navigation experiments in a single real environment. We showed that the reconfigurable maze system can reproduce several existing mazes by recombining the parts of the maze, and that such a transformation can be performed in a short time (~5 min) regardless of the researcher's skill. Furthermore, we conducted behavioral experiments to examine the effects of spatial gaps between the parts of the reconfigurable maze on animal behavior and neural activity. The results suggest that spatial gaps did not alter animal behavior nor did they affect hippocampal neuronal activity. The reconfigurable maze is a system that reproduces maze experiments with multiple shapes in a single environment and provides a means to conduct comparative studies that cannot be performed with conventional mazes.

4.1. Neural recording from freely moving rats

To approximate sensory stimuli to the natural state, animals move freely on runways in a reconfigurable maze. This makes it impossible to record neuronal activity using recording techniques that require the head to be fixed. However, recent advances in recording techniques have made it possible to record neuronal activity in freely moving rats in real environments. Examples include the whole-cell patch clamp method (Lee *et al.*, 2006), Ca²⁺ imaging (Ziv *et al.*, 2013), and neuropixels (Juavinett, Bekheet and Churchland, 2019). In addition, recordings of neuronal activity using traditional tetrodes can be made from animals traversing a ~60 m

maze (Rich, Liaw and Lee, 2014). The combination of these techniques with a reconfigurable maze system can provide additional neurophysiological data.

4.2. Limitations of reproducible maze shapes

The reconfigurable maze reproduces an existing maze shape by placing basic runways on a grid pattern. Therefore, there is a clear limitation to the angles at which the passages can be combined, and the passages can only be arranged in 45° increments, as seen in the radiation maze. Recently, the honeycomb maze has been reported as a maze system capable of performing dynamic deformation (Wood *et al.*, 2018). This is an experimental system in which many hexagonal stages are combined, and each stage is moved up and down by a motor to transform the maze. The honeycomb maze was inspired by Morris's water maze and allowed for 60° navigation, which is not possible with a reconfigurable maze. Because the reconfigurable maze and honeycomb maze are not mutually exclusive, it is possible to realize an additional maze shape by combining them.

In addition, the reconfigurable maze cannot provide a maze shape in which multiple adjacent passages are parallel to one another. This means that the reconfigurable maze cannot directly reproduce the shape of the traditional Hebb-Williams maze (Hebb and Williams, 1946). We can approach the Hebb-Williams maze experiment by using a high wall that prevents animals from entering the next passage, but the introduction of such additional parts may impair the ease and convenience of transforming the reconfigurable maze. For experimental systems that cannot be reconstructed by combining the basic runways, we must consider that they deviate from the range of morphing ability of the reconfigurable maze.

4.3. Morphing runways causes remapping of the place fields

It is well known that the firing position of hippocampal pyramidal cells correlates with the animal's current position, as shown by O'Keefe (O'Keefe and Dostrovsky, 1971). However, it is controversial whether the coordinates represented by the hippocampal place cells are absolute positions in Cartesian coordinates consisting of mutually orthogonal axes. In fact, it has been reported that place cells fire not in absolute coordinates but in relative positions to the runways in morphing such that the angle between runways is changed without changing the total distance of the runways in the W-maze (Dabaghian, Brandt and Frank, 2014). On the other hand, in a morphing experiment using a reconfigurable maze, the total distance of the pathways was kept constant, but the number of curves changed before and after the morphing. The present study suggests that in such morphing, the firing frequency of place cells does not change, and only the location of place fields tends to change. The number of curves may change the running speed of the animal, its angular momentum, and visual cues that be used, but which of these contribute to the remapping of the place fields cannot be determined from the present experimental method.

4.4. Standardization of maze experiments

In recent years, in the field of neuroscience, the lack of reproducibility of animal behavior experiments has become a problem (Botvinik-Nezer *et al.*, 2020). An international research group led by Valeria *et al.* standardized behavioral experiments that could be used in multiple laboratories and reported the results (Aguillon-Rodriguez *et al.*, 2021). In this study, seven research groups shared information on experimental equipment, analysis programs, and

protocols for animal training to standardize experiments on decision-making tasks in head-fixed mice. Although there were differences in the animal behavior learning speeds among the laboratories, there were no significant differences in the results of the animal behavior experiments among the laboratories.

While the reconfigurable maze system allows us to reproduce and compare multiple maze experiments in a single laboratory, standardization requires the sharing of analysis methods and behavioral training protocols among laboratories. Although such efforts are essential for scientific research, they are considered outside the scope of this study. In using the reconfigurable maze system as a general tool for maze experiments, it will be necessary to actively disclose information and to make efforts to standardize behavioral experiments in the future.

4.5. Future Studies

The morphing of the pathway using the reconfigurable maze developed in this study is performed manually and takes ~5 minutes. During this transformation, rats are evacuated from the maze and kept in a specific space. Such a protocol is usual in animal behavioral experiments, but environmental changes may come more quickly in natural conditions. To study neural representations and their remapping in response to such dynamic environmental changes, it is necessary to dynamically transform the passages while the animal is on the maze, as in a honeycomb maze (Wood *et al.*, 2018).

As an accompanying part of a reconfigurable maze, there are movable walls that can dynamically

change the accessibility of a particular runway. This can be used to reproduce experiments that make new pathways available (Poucet and Herrmann, 2001) or block the shortest path (Alvernhe, Save and Poucet, 2011). On the other hand, the honeycomb maze can transform the shape of the maze itself in real time by moving the hexagonal stage up and down using a motor. In the same way, we can realize a dynamic change of the maze shape in the reconfigurable maze system by motor control of the runways and accompanying parts. If we can realize such an automatic reconfigurable maze system, it will be a powerful tool to elucidate the navigation behavior and its neural mechanism against abrupt environmental changes.

5. References

Aguillon-Rodriguez, V. *et al.* (2021) 'Standardized and reproducible measurement of decision-making in mice', *eLife*, 10. doi: 10.7554/ELIFE.63711.

Alvernhe, A., Save, E. and Poucet, B. (2011) 'Local remapping of place cell firing in the Tolman detour task', *European Journal of Neuroscience*, 33(9), pp. 1696–1705. doi: 10.1111/j.1460-9568.2011.07653.x.

Banino, A. *et al.* (2018) 'Vector-based navigation using grid-like representations in artificial agents', *Nature*, 557(7705), pp. 429–433. doi: 10.1038/s41586-018-0102-6.

Bostock, E., Muller, R. U. and Kubie, J. L. (1991) 'Experience-dependent modifications of hippocampal place cell firing', *Hippocampus*, 1(2), pp. 193–205. doi: 10.1002/HIPO.450010207.

Botvinik-Nezer, R. *et al.* (2020) 'Variability in the analysis of a single neuroimaging dataset by many teams', *Nature*, 582(7810), pp. 84–88. doi: 10.1038/s41586-020-2314-9.

Colgin, L. L., Moser, E. I. and Moser, M. B. (2008) 'Understanding memory through hippocampal remapping', *Trends in Neurosciences*, 31(9), pp. 469–477. doi: 10.1016/j.tins.2008.06.008.

Cushman, J. D. *et al.* (2013) 'Multisensory control of multimodal behavior: Do the legs know what the tongue is doing?', *PLoS ONE*, 8(11). doi: 10.1371/journal.pone.0080465.

Dabaghian, Y., Brandt, V. L. and Frank, L. M. (2014) 'Reconceiving the hippocampal map as a topological template', pp. 1–17. doi: 10.7554/eLife.03476.

Deacon, R. M. J. and Rawlins, J. N. P. (2006) 'T-maze alternation in the rodent', *Nature Protocols 2006 1:1*, 1(1), pp. 7–12. doi: 10.1038/nprot.2006.2.

Dombeck, D. A. *et al.* (2010) 'Functional imaging of hippocampal place cells at cellular resolution during virtual navigation', *Nature Neuroscience*, 13(11), pp. 1433–1440. doi: 10.1038/nn.2648.

Eilam, D. and Golani, I. (1989) 'Home base behavior of rats (*Rattus norvegicus*) exploring a novel environment', *Behavioural brain research*, 34(3), pp. 199–211. doi: 10.1016/S0166-4328(89)80102-0.

Foster, D. J. and Wilson, M. A. (2006) 'Reverse replay of behavioural sequences in hippocampal place cells during the awake state', *Nature*, 440(7084), pp. 680–683. doi: 10.1038/nature04587.

Frank, L. M., Brown, E. N. and Wilson, M. (2000) 'Trajectory encoding in the hippocampus and entorhinal cortex', *Neuron*, 27(1), pp. 169–178. doi: 10.1016/S0896-6273(00)00018-0.

Fyhn, M. *et al.* (2004) 'Spatial representation in the entorhinal cortex', *Science*, 305(5688), pp. 1258–1264. doi: 10.1126/SCIENCE.1099901/SUPPL_FILE/FYNH.SOM.PDF.

Harvey, C. D. *et al.* (2009) 'Intracellular dynamics of hippocampal place cells during virtual navigation', *Nature*, 461(7266), pp. 941–946. doi: 10.1038/nature08499.

Harvey, C. D., Coen, P. and Tank, D. W. (2012) 'Choice-specific sequences in parietal cortex during a virtual-navigation decision task', *Nature* 2012 484:7392, 484(7392), pp. 62–68. doi: 10.1038/nature10918.

Hebb, D. O. and Williams, K. (1946) 'A method of rating animal intelligence', *Journal of General Psychology*, 34(1). doi: 10.1080/00221309.1946.10544520.

Hölscher, C. *et al.* (2005) 'Rats are able to navigate in virtual environments', *Journal of Experimental Biology*, 208(3), pp. 561–569. doi: 10.1242/jeb.01371.

Igata, H., Sasaki, T. and Ikegaya, Y. (2016) 'Early Failures Benefit Subsequent Task

Performance', *Scientific Reports*, 6, pp. 1–19. doi: 10.1038/srep21293.

Juavinett, A. L., Bekheet, G. and Churchland, A. K. (2019) 'Chronically implanted neuropixels probes enable high-yield recordings in freely moving mice', *eLife*, 8, pp. 1–17. doi: 10.7554/eLife.47188.

Kennedy, P. J. and Shapiro, M. L. (2009) 'Motivational states activate distinct hippocampal representations to guide goal-directed behaviors', *Proceedings of the National Academy of Sciences of the United States of America*, 106(26), pp. 10805–10810. doi: 10.1073/pnas.0903259106.

Lee, A. K. *et al.* (2006) 'Whole-Cell Recordings in Freely Moving Rats', *Neuron*, 51(4), pp. 399–407. doi: 10.1016/j.neuron.2006.07.004.

Leutgeb, S. *et al.* (2005) 'Neuroscience: Independent codes for spatial and episodic memory in hippocampal neuronal ensembles', *Science*, 309(5734), pp. 619–623. doi: 10.1126/science.1114037.

Lohninger, S., Strasser, A. and Bubna-Littitz, H. (2001) 'The effect of L-carnitine on T-maze learning ability in aged rats', *Archives of Gerontology and Geriatrics*, 32(3), pp. 245–253. doi: 10.1016/S0167-4943(01)00097-8.

Maguire, E. A. *et al.* (2000) 'Navigation-related structural change in the hippocampi of taxi drivers', *Proceedings of the National Academy of Sciences*, 97(8), pp. 4398–4403. doi: 10.1073/PNAS.070039597.

Mathis, A. *et al.* (2018) 'DeepLabCut: markerless pose estimation of user-defined body parts with deep learning', *Nature Neuroscience*, 21(9), pp. 1281–1289. doi: 10.1038/s41593-018-0209-y.

Minderer, M. *et al.* (2016) 'Virtual reality explored', *Nature 2016 533:7603*, 533(7603), pp. 324–325. doi: 10.1038/nature17899.

Muller, R. U. and Kubie, J. L. (1987) 'The effects of changes in the environment on the spatial firing of hippocampal complex-spike cells', *Journal of Neuroscience*, 7(7), pp. 1951–1968. doi: 10.1523/jneurosci.07-07-01951.1987.

Muller, R. U., Kubie, J. L. and Ranck, J. B. (1987) 'Spatial firing patterns of hippocampal complex-spike cells in a fixed environment', *Journal of Neuroscience*, 7(7), pp. 1935–1950. doi: 10.1523/jneurosci.07-07-01935.1987.

O'Keefe, J. and Dostrovsky, J. (1971) 'Short Communications The hippocampus as a spatial

map: Preliminary evidence from unit activity in the freely moving rat', *Brain research*, 34, pp. 171–175.

Olton, D. S. and Samuelson, R. J. (1976) 'Remembrance of places passed: Spatial memory in rats', *Journal of Experimental Psychology: Animal Behavior Processes*, 2(2), pp. 97–116. doi: 10.1037/0097-7403.2.2.97.

Pfeiffer, B. E. and Foster, D. J. (2013) 'Hippocampal place-cell sequences depict future paths to remembered goals', *Nature*, 497(7447), pp. 74–79. doi: 10.1038/nature12112.

Poucet, B. and Herrmann, T. (2001) 'Exploratory patterns of rats on a complex maze provide evidence for topological coding', *Behavioural Processes*, 53(3), pp. 155–162. doi: 10.1016/S0376-6357(00)00151-0.

Quirk, G. J., Muller, R. U. and Kubie, J. L. (1990) 'The firing of hippocampal place cells in the dark depends on the rat's recent experience', *Journal of Neuroscience*, 10(6). doi: 10.1523/jneurosci.10-06-02008.1990.

Ravassard, P. *et al.* (2013) 'Multisensory control of hippocampal spatiotemporal selectivity', *Science*, 340(6138), pp. 1342–1346. doi: 10.1126/SCIENCE.1232655/SUPPL_FILE/RAVASSARD.SM.PDF.

Rich, P. D., Liaw, H. P. and Lee, A. K. (2014) 'Large environments reveal the statistical structure governing hippocampal representations', *Science*, 345(6198), pp. 814–817. doi: 10.1126/science.1255635.

Sharif, F. *et al.* (2021) 'Subcircuits of Deep and Superficial CA1 Place Cells Support Efficient Spatial Coding across Heterogeneous Environments', *Neuron*, 109(2), pp. 363-376.e6. doi: 10.1016/J.NEURON.2020.10.034.

Sharma, S., Rakoczy, S. and Brown-Borg, H. (2010) 'Assessment of spatial memory in mice', *Life Sciences*, 87(17–18), pp. 521–536. doi: 10.1016/j.lfs.2010.09.004.

Skaggs, W. E. *et al.* (1992) 'An Information-Theoretic Approach to Deciphering the Hippocampal Code', *Advances in Neural Information Processing Systems*, 5.

Sofroniew, N. J. *et al.* (2014) 'Natural whisker-guided behavior by head-fixed mice in tactile virtual reality', *Journal of Neuroscience*, 34(29), pp. 9537–9550. doi: 10.1523/JNEUROSCI.0712-14.2014.

Takahashi, S. (2013) 'Hierarchical organization of context in the hippocampal episodic code', *eLife*, 2013(2), pp. 1–17. doi: 10.7554/eLife.00321.

- Thurley, K. and Ayaz, A. (2017) 'Virtual reality systems for rodents', *Current Zoology*, 63(1), pp. 109–119. doi: 10.1093/cz/zow070.
- Tolman, E. C. (1948) 'Cognitive maps in rats and men', *Psychological Review*, 55(4), pp. 189–208. doi: 10.1037/H0061626.
- Tolman, E. C. and Gleitman, H. (1949) 'Studies in spatial learning: VII. Place and response learning under different degrees of motivation', *Journal of Experimental Psychology*, 39(5), pp. 653–659. doi: 10.1037/h0059317.
- Vincent, S. B. (1915) 'The white rat and the maze problem: The introduction of a visual control', *Journal of Animal Behavior*, 5(1), pp. 1–24. doi: 10.1037/H0072410.
- Winocur, G. *et al.* (2010) 'An investigation of the effects of hippocampal lesions in rats on pre- and postoperatively acquired spatial memory in a complex environment', *Hippocampus*, 20(12), pp. 1350–1365. doi: 10.1002/hipo.20721.
- Wood, E. R. *et al.* (2000) 'Hippocampal neurons encode information about different types of memory episodes occurring in the same location', *Neuron*, 27(3), pp. 623–633. doi: 10.1016/S0896-6273(00)00071-4.

Wood, R. A. *et al.* (2018) ‘The honeycomb maze provides a novel test to study hippocampal-dependent spatial navigation’, *Nature*, 554(7690), pp. 102–105. doi: 10.1038/nature25433.

Zhang, K. *et al.* (1998) ‘Interpreting Neuronal Population Activity by Reconstruction: Unified Framework With Application to Hippocampal Place Cells’, *Journal of Neurophysiology*, 79(2), pp. 1017–1044. doi: 10.1093/cercor/6.3.406.

Ziv, Y. *et al.* (2013) ‘Long-term dynamics of CA1 hippocampal place codes’, *Nature Neuroscience*, 16(3), pp. 264–266. doi: 10.1038/nn.3329.